Unexpected diversity of *Isidoides* (Anthozoa: Octocorallia: Isidoidae) revealed by morphology and phylogenomics analysis with descriptions of four new species

Yu Xu[1,†], Jaret P. Bilewitch[2,†], Eric Pante[3,4,†], Zifeng Zhan[1], Sadie Mills[2], Malcolm R. Clark[2] and Kuidong Xu[1,5,*]

[1] Laboratory of Marine Organism Taxonomy and Phylogeny, Qingdao Key Laboratory of Marine Biodiversity and Conservation, Shandong Province Key Laboratory of Experimental Marine Biology, Institute of Oceanology, Chinese Academy of Sciences, Qingdao 266071, China
[2] New Zealand Institute of Earth Science Ltd (NZIES), 301 Evans Bay Parade, Wellington 6021, New Zealand
[3] Univ Brest, CNRS, IRD, Ifremer, UMR 6539, LEMAR, Plouzané, France
[4] Institut Systématique Evolution Biodiversité (ISYEB), Muséum national d'Histoire naturelle, CNRS, Sorbonne Université, EPHE, Université des Antilles, 43 rue Cuvier, CP 26, 75005 Paris, France
[5] University of Chinese Academy of Sciences, Beijing 100049, China

*Corresponding author: Kuidong Xu
Correspondence: kxu@qdio.ac.cn
[†]These authors contributed equally to this work

ABSTRACT

Isidoidae Heestand Saucier, France & Watling, 2021 is a rare octocoral family currently represented by a single genus and species, *Isidoides armata* Nutting, 1910 recorded in the western Pacific Ocean. The taxonomic status and diversity of *Isidoides* remain unclear, due to the lack of diagnostic taxonomic features and limited taxon sampling. Based on 23 *Isidoides* specimens obtained from the northwestern to southwestern Pacific, we carried out morphological and phylogenetic analyses to reveal the taxonomic status of species and develop reliable features for species identification. The 23 specimens could be classified into five well-separated groups by the phylogenomic analysis of ultraconserved elements (UCEs), four groups by *28S rDNA*, and two groups by *mtMutS-cox1*. Integrating morphology and molecular data, we uncovered unexpected diversity of Isidoides composed of the known species *Isidoides armata* and four new species, viz., *I. elegans* sp. nov., *I. gracilis* sp. nov., *I. incrassata* sp. nov. and *I. pseudarmata* sp. nov. The morphological analysis showed high intraspecific morphological variation in colony color and the size, shape and arrangement of polyps. By contrast, the sclerite forms with their surface sculpturing are more reliable features for species identification. Our phylogenetic analyses indicate that UCE phylogenomics has higher resolution than the nuclear *28S rDNA* and the mitochondrial genes *mtMutS* and *cox1* for species delimitation within Isidoidae.

Keywords: deep sea, *Isidoides*, new species, phylogeny, Scleralcyonacea, seamount, taxonomy, ultraconserved elements

Introduction

Octocorals are often the key megafauna in deep-sea benthic ecosystems with hard substrate, for instance seamounts, where they may form coral forests and serve as vital habitats for marine life (e.g., Krieger and Wing, 2002; Buhl-Mortensen and Mortensen, 2005; Parimbelli, 2020; Rossi et al., 2022; Morrissey et al., 2023). With their significant ecological value and fragility, octocorals have been considered an indicator group for the conservation of vulnerable marine ecosystems, particularly the ecosystems on seamounts (Dautova, 2019; Watling and Auster, 2021). Historically, octocoral taxonomy has relied exclusively on morphological traits (e.g., Bayer, 1981). Recent advances in molecular methods have prompted major revisions to their classification (McFadden et al., 2022). Nevertheless, challenges in octocoral systematics persist, and the biodiversity of many groups is still largely unknown (Kessel et al., 2022).

Isidoidae Heestand Saucier, France & Watling, 2021 is a rare octocoral group comprising only the monotypic genus *Isidoides* Nutting, 1910, with the species *I. armata* Nutting, 1910 recorded from the tropical western Pacific Ocean (Nutting, 1910). The genus has been assigned to various families, including Chrysogorgiidae, Ellisellidae, Primnoidae and Isididae, due to its obscure morphological features (Bayer, 1979; Bayer and Stefani, 1988; Bayer and Grasshoff, 1994). The molecular phylogenetic study of Pante et al. (2013) showed a close affinity between *Isidoides* and the Isididae subfamily Keratoisidinae (now elevated to family Keratoisididae), but placed the genus as *incertae sedis*. Later, the family Isidoidae was established to contain the genus *Isidoides* with a non-articulated axis and a distinct sclerite form, based on the phylogenetic analysis of *mtMutS* + *18S rDNA* and a unique arrangement of mitochondrial genes (Heestand Saucier et al., 2021). The phylogenomic analysis of ultraconserved elements (UCEs) corroborated the validity and distinctiveness of the family Isidoidae, showing a sister relationship with Keratoisididae (e.g., McFadden et al., 2021, 2022).

When re-examining the collections Pante et al. (2013) found that the holotype (a fragment) of *I. armata* illustrated in Nutting (1910) was lost but another fragment from a different locality was found. To avoid future taxonomic confusion, Pante et al. (2013) designated Nutting's illustrated (but lost) fragment as the lectotype, and the existing fragment as a paralectotype. Nonetheless, they could not assert whether the holotype and the alternative fragment originated from the same colony. Meanwhile, they succeeded in obtaining *mtMutS* gene sequences from newly collected specimens from New Caledonia and New Zealand and revealed three haplotypes (A, B and C). Pante et al. (2013) suggested that the paralectotype of *I. armata* and the specimens representing the three haplotypes could represent four species. They noted that the paralectotype differs from the New Caledonia and New Zealand specimens in having more slender polyps and a thinner, transparent coenenchyme, and that specimens with haplotype C possess a distinctive dark golden-brown to black axis. However, the available data were insufficient to separate these specimens, which were conservatively treated as *Isidoides armata* (Pante et al., 2013).

The 5'-end of the mitochondrial gene *mtMutS* has been commonly used in the molecular identification of octocorals, and multilocus barcodes (*mtMutS* + *cox1*) can discriminate roughly 70% of octocoral morphospecies (e.g., McFadden et al., 2010, 2011; McFadden and van Ofwegen, 2013). A single mutation at *mtMutS* has been used to separate species (Pante and Watling, 2012; Pante et al., 2015). However, in many cases, both the loci *mtMutS* and *cox1* are too conserved for species delimitation. For example, concatenated *mtMutS-cox1* could not discriminate the congeners *Chrysogorgia pendula*, *C. acanthella* and *C. cylindrata* (Xu et al., 2023). The nuclear *28S rDNA* gene has shown a higher level of genetic variation among chrysogorgiid species and has been proposed as a potential barcode for octocoral species delimitation (Xu et al., 2021a, b; Baena et al., 2024). Recently, ultraconserved elements (UCEs) and exons obtained from target-capture enrichment and genome skimming have offered advantages over traditional Sanger sequencing and other next-generation sequencing methods such as RAD-seq, as they can address a wide range of evolutionary and taxonomic questions across deep to shallow timescales within the Anthozoa (Quattrini et al., 2017; Erickson et al., 2020; Untiedt et al., 2021). However, UCEs have primarily been used to confirm the relationship between higher-level taxa (e.g., McFadden et al., 2022), and so far, have rarely been used for separation and identification of species (e.g., Erickson et al., 2020; Untiedt et al., 2021).

In this study, we examined the specimens of *Isidoides* collected from the northwestern to the southwestern Pacific, and used DNA sequencing analyses of barcode and UCE loci to reveal the taxonomy

and diversity of *Isidoides* Nutting, 1910. Based on examination of historical and newly collected specimens, we review and revise the genus *Isidoides*.

Material and methods

Specimen collection and morphological examination

Six specimens were collected in the tropical western Pacific during cruises of the R/V *KeXue* (Science) using the ROV *FaXian* (Discovery) and an electro-hydraulic grab. Of these, four specimens of *I. gracilis* sp. nov. were collected in the South China Sea in 2016, 2018 and 2022, and two specimens of *I. elegans* sp. nov. were collected in 2019 from an unnamed seamount on the Caroline Ridge. *In-situ* photographs of the specimens were taken by the ROV before sampling, whenever possible. After collection, all specimens were photographed on-board and in the laboratory and were preserved in 75% ethanol for further morphological and molecular analyses. Five specimens of *I. pseudarmata* sp. nov. and ten specimens of *I. armata* were sourced from the Muséum national d'Histoire naturelle (Paris, France); One specimen of *I. armata* and one specimen of *I. incrassata* sp. nov. were sourced from the NIWA Invertebrate Collection (Wellington, New Zealand); all of which were collected from New Caledonia to New Zealand.

Morphological terminology follows Bayer et al. (1983). Scanning electron microscopy (SEM) preparation of polyps and sclerites follow the procedures in Xu et al. (2023). The type and voucher specimens of *I. gracilis* sp. nov. and *I. elegans* sp. nov. have been deposited in the Marine Biological Museum of the Chinese Academy of Sciences (MBMCAS) at Qingdao, China. The types of *I. pseudarmata* sp. nov. are deposited in the Muséum national d'Histoire naturelle in Paris, France. The types of *Isidoides incrassata* sp. nov. are deposited in the NIWA Invertebrate Collection in Wellington, New Zealand.

DNA extraction and Sanger DNA sequencing

The TIANamp Marine Animal DNA Kit (Tiangen Biotech, Beijing, China) was used to extract total genomic DNA from polyp tissue. Sequences of the mitochondrial genes *mtMutS* and *cox1*, and the nuclear gene *28S rDNA* were obtained through Sanger sequencing of polymerase chain reaction products for molecular systematic analysis. To amplify *mtMutS*, *cox1* and *28S*, the primer pairs AnthoCorMSH (Herrera et al., 2010) and Mut-3458R (Sánchez et al., 2003), COI8414-F (McFadden, unpublished) and HCO2198 (Folmer et al., 1994), 28S-Far/28S-Rar (McFadden and van Ofwegen, 2013) were used, respectively. PCR conditions were: 2 min at 98 °C followed by 35 cycles (98 °C for 15 s, 45–50 °C for 15 s, and 72 °C for 60 s) and a final extension at 72 °C for 2 min. PCR products were sent to TsingKe Biotech (Beijing, China) for bidirectional sequencing using the corresponding forward and reverse primer. All newly obtained sequences were deposited on NCBI Genbank (Table 1).

Genetic distance and phylogenetic analyses of Sanger sequencing

Additional *mtMutS*, *cox1* and *28S rDNA* sequences of the genus *Isidoides*, Keratoisididae and Chrysogorgiidae were obtained from Genbank (Table 1). MAFFT v.7 (Katoh and Standley, 2013) with the G-INS-i algorithm was used to align the sequences and BioEdit v7.0.5 (Hall, 1999) was used to refine the nucleotide alignment. Genetic distances, calculated as uncorrected "p" distances within-and among species, were estimated using MEGA 11 (Tamura et al., 2021).

Bayesian Inference (BI) and Maximum Likelihood (ML) were used to generate phylogenetic trees of the *mtMutS-cox1* and *28S rDNA* genes. Model selection, Maximum likelihood (ML) and Bayesian inference (BI) analyses were conducted by PhyloSuite v1.2.2 (Zhang et al., 2020; Xiang et al., 2023). The best partitioning scheme and evolutionary models for *mtMuts* and *cox1* were selected for ML using PartitionFinder2 v2.1.1 (Lanfear et al., 2017), with the greedy algorithm and AICc criterion. ModelFinder v2.2.0 (Kalyaanamoorthy et al., 2017) was used to select the best-fit model for BI using the BIC criterion. HKY+F+G4 was selected as the best-fit substitution model for both the *mtMutS-cox1* and *28S rDNA* alignments. Bayesian Inference (BI) phylogenies were inferred using MrBayes 3.2.7a (Ronquist et al., 2012) using two parallel runs of 10^7 generations, with 25% of sampled generations discarded as burn-in. Convergence of the MCMC runs was evaluated based on summary statistics in PhyloSuite v1.2.2.

Maximum likelihood (ML) phylogenies were inferred using IQ-TREE v (Nguyen et al., 2015) with 1,000 standard bootstrap replicates. Following Hillis and Bull (1993), the ML bootstraps <70%, 70–94% and ≥95% were considered low, moderate and high, respectively. Following Alfaro et al. (2003), the Bayesian posterior probabilities <0.95 and ≥0.95 were considered low and high, respectively.

Abbreviations used in this paper include:

BI: Bayesian Inference
MBMCAS: Marine Biological Museum, Chinese Academy of Sciences, Qingdao, China
ML: Maximum Likelihood
MNHN: Muséum national d'Histoire naturelle, Paris, France
SEM: Scanning Electron Microscope
UCEs: ultraconserved elements

Table 1. The sequences used in this study. New species with their sequences in this study are in bold. "–" means unavailable data.

Species	Voucher	Isolate number	GenBank Accession numbers			
			mtMutS	*cox1*	*28S rDNA*	UCEs (SRA)
***Isidoides elegans* sp. nov.** (holotype)	MBM286500	M5223	**PV926094**	**PV915943**	**PV919767**	**SAMN50046240**
***I. elegans* sp. nov.** (paratype)	MBM286501	M5043	**PV926093**	**PV915942**	**PV919768**	**SAMN50046241**
***I. gracilis* sp. nov.** (holotype)	MBM286877	Z076	**PV926096**	**PV915945**	**PV919769**	**SAMN50046242**
***I. gracilis* sp. nov.** (paratype)	MBM286878	N11	**PV926095**	**PV915944**	–	**SAMN50046243**
***I. gracilis* sp. nov.** (paratype)	MBM286879	RY16049	**PV926098**	**PV915946**	**PV919766**	**SAMN50046244**
***I. gracilis* sp. nov.** (paratype)	MBM286880	RY16141	**PV926097**	**PV915947**	**PV919763**	**SAMN50046245**
***I. incrassata* sp. nov.** (holotype)	NIWA163516	MBM286882	**PV926100**	**PV915949**	**PV919764**	**SAMN50046247**
I. armata	NIWA82680	MBM286881	**PV926099**	**PV915948**	**PV919765**	**SAMN50046246**
I. armata	MNHN-IK-2008-1510	TER20516	JN227946, **PV926086**	JN227951, KX530099, **PV915935**	–	**SAMN50046232**
I. armata	AM:G16995	NORF3610	JN228002	–	–	–
I. armata	MNHN-IK-2009-1632	CP38321	KX362340, **PV926090**	**PV915939**	**PV919757**	**SAMN50046236**
I. armata	MNHN-IK-2008-1505	TER105-1	JN227934, **PV926081**	**PV915930**	**PV919752**	**SAMN50046227**
I. armata	–	–	NC_062015	NC_062015	–	–
I. armata	–	–	OL616240	OL616240	–	–
I. armata	MNHN-IK-2008-1506	–	**PV926082**	**PV915931**	**PV919753**	**SAMN50046228**
I. armata	MNHN-IK-2016-2540	–	**PV926092**	**PV915941**	**PV919762**	**SAMN50046239**
I. armata	MNHN-IK-2016-2539	–	**PV926091**	**PV915940**	**PV919761**	**SAMN50046238**
I. armata	MNHN-IK-2008-1411	NOR220652	**PV926079**	**PV915928**	**PV919750**	**SAMN50046225**
I. armata	MNHN-IK-2008-1504	TER1012	**PV926080**	**PV915929**	**PV919751**	**SAMN50046226**
I. armata	MNHN-IK-2008-1507	TER10084	**PV926083**	**PV915932**	**PV919754**	**SAMN50046229**
I. armata	MNHN-IK-2011-1000	–	–	–	–	**SAMN50046237**
***I. pseudarmata* sp. nov.** (paratype, "*I. armata*" in Pante et al. 2013)	MNHN-IK-2008-1875	TER1021	KX362253, **PV926089**	**PV915938**	**PV919760**	**SAMN50046235**
***I. pseudarmata* sp. nov.** (paratype, "*I. armata*" in Pante et al. 2013)	MNHN-IK-2008-1867	TER1061	JX126866, **PV926087**	**PV915936**	**PV919758**	**SAMN50046233**
***I. pseudarmata* sp. nov.** (paratype)	MNHN-IK-2008-1508	–	**PV926084**	**PV915933**	**PV919755**	**SAMN50046230**
***I. pseudarmata* sp. nov.**	MNHN-IK-2008-	–	**PV926085**	**PV915934**	**PV919756**	**SAMN50046231**

(paratype)	1509					
***I. pseudarmata* sp. nov.** (holotype)	MNHN-IK-2008-1869	–	**PV926088**	**PV915937**	**PV919759**	**SAMN50046234**
Parajasonisis flabellata	MBM287336	M1003	PP999495	PP991392	PP992072	–
Parajasonisis flabellata	MBM287337	M1155	PP999496	PP991393	PP992073	–
Dentatisis bathyalis	MBM287339	M088	PP999498	PP991395	PP992075	–
Dentatisis projecta	RSIOOC0210	JL171-B10	PP999497	PP991394	PP992074	–
Aethisis turriformis	RSIOOC0241	JL179-B05	PP999499	PP991396	PP992076	–
Jasonisis thresheri	TMAG K3879	OCT052	JN620806	JN620807	–	–
Dokidisis krishanani	NCPOR/HYD-CIOR/0070	–	OQ594413	OQ605881	OQ625531	–
Cladarisis nouvianae	YPM IZ 070870	RUM1072	KX362252	KX530100	–	–
Keratoisis grayi	CMNI 2021-0118	–	KX362308	KX530101	–	–
Adinisis oblonga	NCPOR/HYD-CIR/0086	–	OQ594412	OQ605880	OQ625532	–
Keratoisididae sp. S1	MBM287343	Z5064	PQ268061	PQ248516	PQ249238	–
Keratoisididae sp. I1	MBM287345	YM042	PQ268063	PQ248518	PQ249240	–
Keratoisididae sp. I4	MBM287348	YM213	PQ268066	PQ248521	PQ249243	–
Keratoisididae sp. D2	MBM287352	M8088	PQ268070	PQ248525	PQ249247	–
Keratoisididae sp. C1	MBM288057	10-4	PQ268076	PQ248531	PQ249253	–
Keratoisididae sp. H1	MBM288065	10-12	PQ268085	PQ248540	PQ249262	–
Chrysogorgia averta	LII-10-609	–	KC788265	KC788235	KC788258	–
Chrysogorgia arboriformis	MBM286465	–	ON221842	ON207094	ON207672	–
Parachrysogorgia chrysei	MBM286358	–	ON221840	ON207090	ON207678	–
Radicipes stonei	USNM:IZ:1418007/SW0714	–	MG986912	MG986961	MG980134	–

DNA Target Enrichment and Sequencing

Twenty-three specimens were selected for DNA sequencing of UCEs using target bait enrichment, as per Quattrini et al. (2017). DNA extracts were sent to Bluescape Hebei Biotech Co. Ltd. (Baoding P.R. China) for target enrichment and library preparation. The library was sequenced by Novogene Co., Ltd. (Beijing) on an Illumina Novaseq X Plus platform; raw sequence reads were deposited in the NCBI Sequence Read Archive (SRA) (https://www.ncbi.nlm.nih.gov/sra) as BioProject PRJNA1293818. The resulting fastq files were processed using *phyluce* v1.7.3 (Faircloth, 2015) according to Quattrini et al. (2017), except that contigs were assembled with *SPAdes* v.4.0.0 (Bankevich et al., 2012) using the 'single-cell' assembly mode without the 'careful' option. After matching UCEs to the "octocoral-v2" bait set (Erickson et al., 2020), sequence data from three keratoisidid outgroup specimens were obtained from previous studies (McFadden et al., 2022; A. Quattrini pers. comm.) and were included in subsequent alignments and phylogenetic analyses. Final concatenated matrices included loci with 75% and 90% taxon occupancy (i.e., the proportion of taxa represented per locus). Each alignment was analyzed independently using *ExaBayes* v1.5.1 (Aberer et al., 2014), with partitioning by locus, using four chains of 10^6 generations sampled every 1,000 generations. Phylogenetic reconstruction used 90% of the resulting samples, discarding the first 10% as burn-in.

Results

Genetic distance and phylogenetic analyses of Sanger sequencing

The new sequences, including 22 *mtMutS*, 22 *cox1* and 20 *28S rDNA*, were obtained successfully from 23 specimens and deposited in GenBank (Table 1). The alignments comprised 808, 540 and 682 bp nucleotide positions for the *mtMutS*, *cox1* and *28S rDNA* regions, respectively. The *mtMutS-cox1* data had 7011 bp indels and 2982 bp external gap; *28S rDNA* data contained 1548 bp indels with 82 bp external gap. Based on these alignments, the *mtMutS-cox1* and *28S* rDNA interspecific distances among the *Isidoides* species

ranged from 0–0.34% and 0–3.46%, respectively, and the corresponding intraspecific distances were 0–0.08% and 0–0.47% (Tables 2, 3).

The ML tree was nearly identical in topology to the BI tree, and thus a single tree with both support values is presented for concatenated *mtMutS-cox1* and *28S rDNA* (Figs. 1, 2). All the *Isidoides* species formed a monophyletic group in both the *mtMutS-cox1* and *28S* rDNA trees with high to full branch support. In the *mtMutS-cox1* trees (Fig. 1), two specimens of *I. elegans* sp. nov. formed a single clade with high support in the BI tree (BI posterior probability = 0.98), and were sister to *I. gracilis* sp. Nov., albeit with low support. *Isidoides pseudarmata* sp. nov. and *I. incrassata* sp. nov. clustered with *I. armata* species with low support.

In the *28S rDNA* trees (Fig. 2), two specimens of *I. elegans* sp. nov. formed a single clade with high to full branch support in both the ML and BI trees (BI posterior probability =1.00, ML bootstrap = 100). Three specimens of *I. gracilis* sp. nov. formed a single clade with moderate to high support in the BI and ML trees (BI = 0.89, ML = 99), and this clade was sister to *I. elegans* sp. nov. Five specimens of *I. pseudarmata* sp. nov. formed a single clade with full and moderate support in the BI and ML trees (BI = 1.00, ML = 91), respectively. *Isidoides incrassata* sp. nov. clustered with *I. armata* with low support.

Table 2. The sequences used in this study. New species with their sequences in this study

	Species	1	2	3	4	5
1	*Isidoides armata* (MNHN-IK-2008-1504, 2008-1505, 2008-1506, 2009-1632, 2016-2539, NIWA82680, NORF3610, TER1051, NC062015, OL616240, CP38321), *Isidoides pseudarmata* sp. nov. (MNHN-IK-2008-1508, 2008-1509, 2008-1867, 2008-1869, 2008-1875, TER1021, TER1061), *Isidoides incrassata* sp. nov. NIWA163516,	0				
2	*Isidoides armata* (MNHN-IK-2008-1411, 2008-1507, 2008-1510, 2016-2540)	0.08	0			
3	*Isidoides gracilis* Z076, 11, RY16049, RY16141	0.08	0.17	0		
4	*Isidoides elegans* M5043, M5223	0.17	0.25	0.08	0	
5	*Isidoides armata* TER20516	0.17	0.08	0.25	0.34	-

Table 3. Inter- and intraspecific uncorrected pairwise (p) distances at 28S rDNA of Isidoidae species (%).

	Species	1	2	3	4	5	6	7	8	9	10	11
1	*Isidoides armata* MNHN-IK-2008-1505, 2008-1506, *I. incrassata* sp. nov. NIWA163516	0										
2	*I. armata* MNHN-IK-2008-1504	0.16	-									
3	*I. armata* MNHN-IK-2008-1507, 2016-2540, NIWA82680	0.16	0.31	0								
4	*I. armata* MNHN-IK-2008-1632, 2016-2539	0.31	0.16	0.16	0							
5	*I. armata* MNHN-IK-2008-1411	0.31	0.47	0.16	0.31	-						
6	*I. pseudarmata* sp. nov. MNHN-IK-2008-1509, 2008-1867, 2008-1869	0.63	0.79	0.47	0.63	0.63	0					
7	*I. pseudarmata* sp. nov. MNHN-IK-2008-1508	0.79	0.94	0.63	0.79	0.79	0.16	-				
8	*I. pseudarmata* sp. nov. MNHN-IK-2008-1875	0.94	1.10	0.79	0.94	0.94	0.31	0.16	-			
9	*Isidoides gracilis* sp. nov. RY16141, RY16049, Z076	2.52	2.68	2.36	2.52	2.52	2.83	2.99	2.83	0		
10	*Isidoides elegans* sp. nov. M5223	2.83	2.99	2.68	2.83	2.83	3.15	3.31	3.15	0.94	-	
11	*I. elegans* sp. nov. M5043	2.99	3.15	2.83	2.99	2.99	3.31	3.46	3.31	1.10	0.16	-

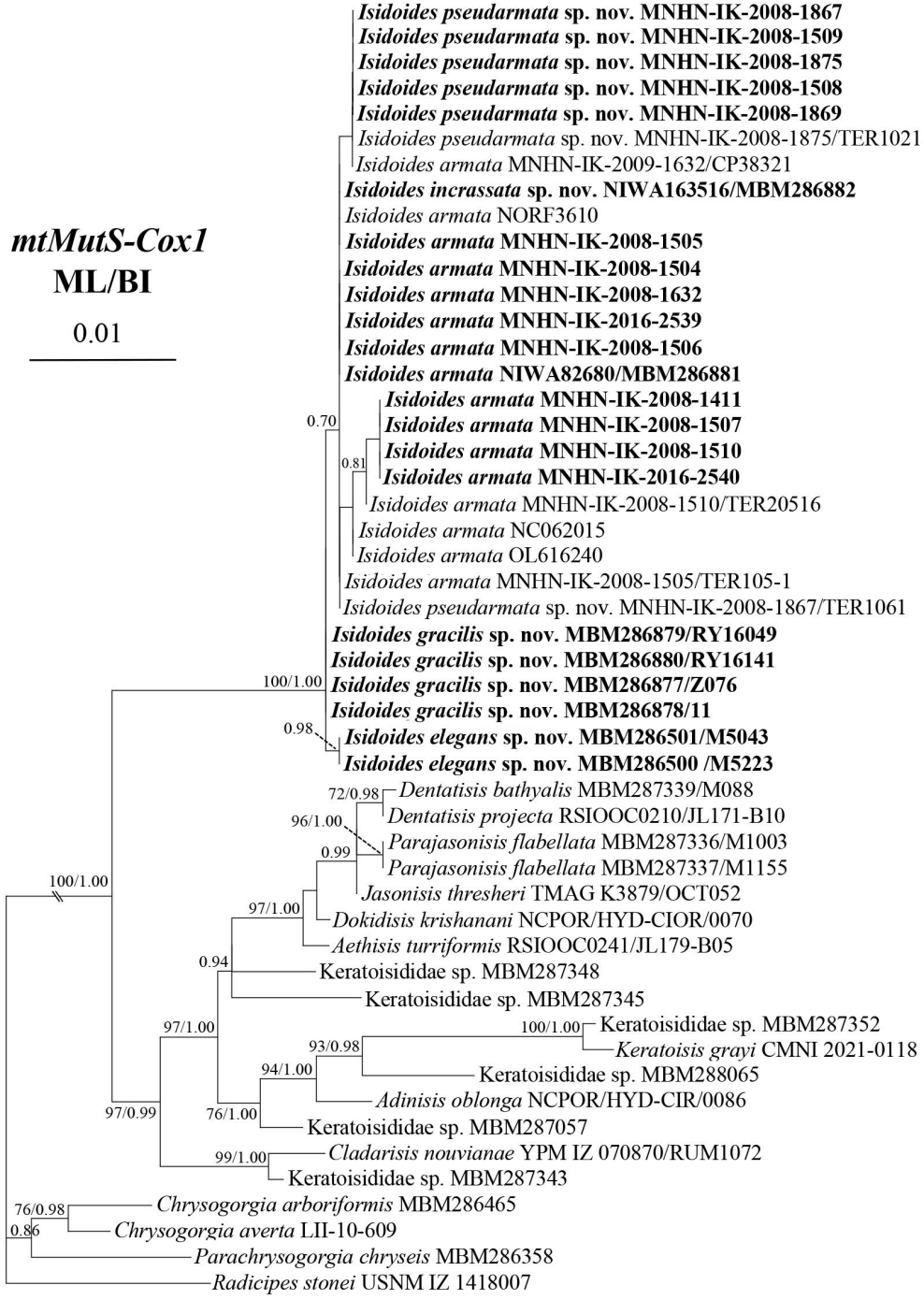

Figure 1 ML tree of the *mtMutS-cox1* marker showing phylogenetic relationships among the isidoid, keratoisidid and chrysogorgiid species. The BI tree is identical to the ML tree in topology. BI posterior probabilities (after slash) and ML bootstrap values (before slash) are shown on each node. Branches with ML bootstrap <70% or BI posterior probability <0.70 do not display support values. Chrysogorgiidae species are used as the outgroup. Voucher/isolate numbers are listed at the right-hand side of the cladogram. The specimens with sequences generated in this study are presented in bold.

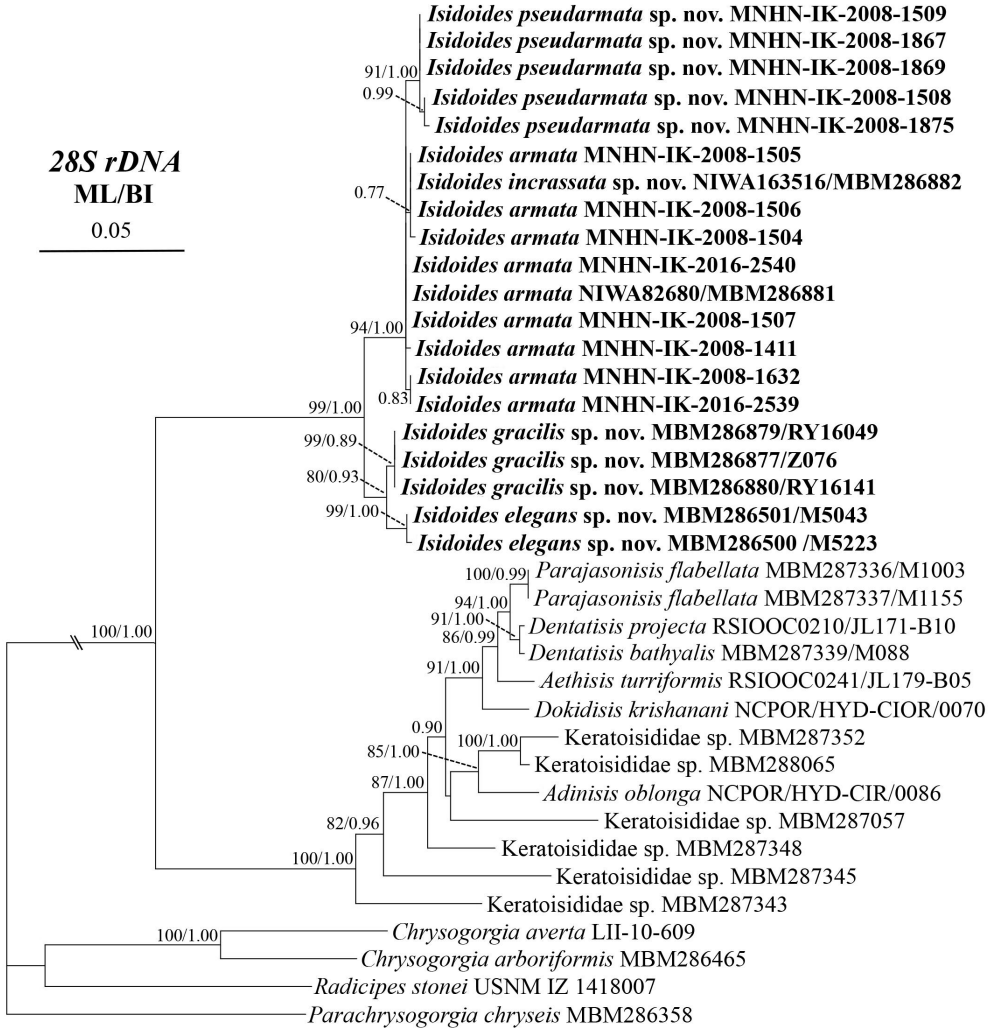

Figure 2 ML tree of the *28S* gene showing phylogenetic relationships among the isidoid, keratoisidid and chrysogorgiid species. The BI tree is identical to the ML tree in topology. BI posterior probabilities (after slash) and ML bootstrap values (before slash) are shown on each node. Nodes with ML bootstrap <70% or BI posterior probability <0.70 do not show support values. The out groups are the species of Chrysogorgiidae. Voucher/isolate number are listed at the right side of the cladogram. The specimens with their sequences in this study are in bold.

Figure 3 Bayesian phylogenetic tree reconstructed from a concatenated UCE dataset for *Isidoides* specimens, where only loci with at least 75% of all taxa represented were included (75%-occupancy). All branches had 100% posterior probability support. The tree was rooted using three keratoisidids . A tree reconstructed from a 90%-occupancy alignment produced identical results, except that specimen 2008-1510 (indicated by an arrow) instead formed a sister-relationship with MBM286881.

Phylogenomic analysis of UCEs sequences

After quality-based trimming, the number of reads generated for target-enriched sequences ranged from 5,052,234 to 28,465,519 for each of the 23 *Isidoides* specimens. Trimmed reads were assembled *de novo* into an average of 125,486 (SE=16,877) contigs per sample, with a range of 32,906 to 295,268. Matching to the *octocoral-v2* baitset resulted in the recovery of 176 to 2,250 UCE loci ($\bar{x}$=1788, SE=109). Two specimens that produced fewer than 1000 UCE loci (2011-1000, 2016-2539) were discarded from further analysis, leaving sequence data for 21 specimens that were concatenated to produce final alignments of 933,572 bp for 1,575 loci (75% occupancy) and 430,746 bp for 762 loci (90% occupancy). Multi-locus Bayesian phylogenetic analysis of each alignment produced topologies that were identical except for the placement of a single specimen (Fig. 3).

Tree topologies for the UCE analysis distinguished five well-supported clades, corresponding to *I. armata* plus four new species described herein. The UCE analysis resolved *I. gracilis* sp. nov. and *I. elegans* sp. nov. as monophyletic clades, as seen in the *mtMutS-cox1* tree (for *I. elegans* sp. nov.: Fig. 1) and the *28S* tree (for both species: Fig. 2), and fully resolved the relationships among *I. armata*, *I. pseudarmata* sp. nov., and *I. incrassata* sp. nov., which formed a polytomy in both single-locus gene trees. Further subdivisions within each of these clades were also well-supported but morphological analysis was unable to identify discriminating characters and as such these genetic differences were interpreted as intraspecific variation within the proposed species diagnoses.

Systematics

Taxonomy

Phylum Cnidaria Hatschek, 1888
Subphylum Anthozoa Ehrenberg, 1834
Class Octocorallia Haeckel, 1866
Order Scleralcyonacea McFadden, van Ofwegen & Quattrini, 2022
Family Isidoidae Heestand Saucier, France & Watling, 2021

Genus *Isidoides* Nutting, 1910

Diagnosis (Based on Heestand Saucier et al. 2021): Colony planar with pseudo-dichotomous branching, sometimes covered with a layer of thick tegument on surface. Axis solid and calcareous, white to dark golden-brown, not articulated, occasionally flattened along the face of the fan. Polyps non-retractile, large and tubular or small and wart-like, sometimes distally expanded, arranged biserially or irregularly on all sides of the axis. Sclerites as flattened rods to rods with relatively uniform shape, occasionally cross-shaped. Sclerites of coenenchyme surface compact and uniform, some densely granulated. Sclerites abundant and tightly packed on the polyp and coenenchyme, but absent from the pharynx.

Type species: *Isidoides armata* Nutting, 1910.

Distribution: Indo-West Pacific and southwest Pacific, 424–1065 m (Table 4; Nutting 1910, Pante *et al.* 2013, and present study).

***Isidoides armata* Nutting, 1910**
Fig. 4D, G, L, M, O; 5A–C, 6–12

Isidoides armata Nutting, 1910: 33–34, Plate VIII, figs. 2, 2a, Plate XI, fig. 5.
Isidoides armata: Pante et al. 2013, 371–374, figs. 2–4, 8–10.

Material examined: Paralectotype: ZMA Coel. 02711. Other specimens: MNHN-IK-2008-1505, 2008-1411, 2008-1504, 2009-1632, 2008-1507, 2008-1506, 2008-1510, 2016-2540, 2016-2539, 2011-1000 and AM G.16995 in Muséum national d'Histoire naturelle in Paris, France; NIWA 82680 in NIWA Invertebrate Collection in Wellington, New Zealand. The collection information of these specimens is listed in Table 5.

Diagnosis. Colony planar with irregular pseudo-dichotomous branching and white, light brown or brown color after collection. Axis white to light brown, occasionally flattened. Polyps vary greatly in size, shape, and thickness, and can be large and tubular or club-shaped with thick or translucent tissues, sometimes curved, or small and conical or wart-like. Polyps biserially or irregularly arranged around the axis, sometimes absent on the back of the colony. Tentacles tightly folded over the oral disk forming a pseudo-operculum, with the polyp head sometimes expanded. All sclerites with granulated or ridged surface and two rounded ends, occurring as rods in tentacles, and flattened rods in polyp body wall and coenenchyme, some of them scale-like with a slightly medial constriction.

Morphology of *I. armata* form 1 (lectotype, Fig. 5A, based on Nutting 1910): Colony and axis both very light brown. Axis solidly calcareous and round. Branches irregularly and pseudo-dichotomously branched. Polyps usually irregularly arranged on two sides of the main branches, sometimes on all side of the terminal branchlets, averaging about 2 mm apart. The individual polyps vary greatly in size and shape, but with the distal ends almost always enlarged (bud-like), about 1.4 mm in diameter. Single polyp tubular with mostly 1.8 mm in height when retracted, and club-shaped up to 4 mm when expanded. Sclerites all bar-like with a smooth profile and two rounded ends, often being somewhat expanded distally. Their surface with a very fine, dense, granulated appearance. Bar-like or lenticular sclerites criss-cross arranged on polyp body wall, but tend to be vertical when polyp expanded and horizontal when retracted, especially near the margin. Tentacles closely folded over the oral disk forming a pseudo-operculum and covered with longitudinally arranged bar-like sclerites.

Table 4. The sampling localities of included *Isidoides* specimens. Some records were obtained from Nutting 1910 and Pante et al. 2013. "–" = unknown data.

Species	Isolate number	Voucher number	haplotype	Sampling location	Depth (m)	Latitude	Longitude	Collection date
Isidoides armata Nutting, 1910 (lectotype)	–	–	-	Eastern slope of Elat, Kei Islands, Arafura Sea	984	–5.900	132.945	20/12/1899
I. elegans sp. nov. (holotype)	M5043	MBM286500	-	An unnamed seamount on the Caroline Ridge	814	10.076	140.190	31/5/2019
I. elegans sp. nov. (paratype)	M5223	MBM286501	-	An unnamed seamount on the Caroline Ridge	962	10.078	140.203	27/5/2019
I. gracilis sp. nov. (paratype)	11	MBM286878	-	Ganquan Plateau, South China Sea	586–910	–	–	14/6/2018
I. gracilis sp. nov. (holotype)	Z076	MBM286877	-	Zhenbei Seamount, South China Sea	797	15.049	116.558	20/7/2022
I. gracilis sp. nov. (paratype)	RY16049	MBM286879	-	Northern South China Sea	811	22.035	118.776	–/9/2016
I. gracilis sp. nov. (paratype)	RY16141	MBM286880	-	Northern South China Sea	–	22.035	118.776	–/9/2016
I. incrassata sp. nov. (holotype)	NIWA163516	MBM286882	-	Bay of Plenty, New Zealand	614	–37.1	177.3	13/08/1998
I. armata Nutting, 1910	NIWA82680	MBM286881	-	Bay of Plenty, New Zealand	878	–36.81	177.47	22/04/2012
I. armata Nutting, 1910	NORF36/10	AM G.16995	A	North of Norfolk Island, Norfolk Ridge, Australia	1035–1065	–28.520	167.790	17/05/2003
I. armata Nutting, 1910	NOR220652	MNHN-IK-2008-1411	A/C	Athos Seamount, Norfolk Ridge, New Caledonia	750–800	–25.267	168.933	26/10/2003
I. armata Nutting, 1910	TER1051	MNHN-IK-2008-1505	A	Walpole Island, Loyalty Ridge, New Caledonia	790–800	–22.687	168.942	16/10/2008
I. armata Nutting, 1910	TER1012	MNHN-IK-2008-1504	A	Walpole Island, Loyalty Ridge, New Caledonia	720	–22.675	168.962	16/10/2008
I. armata Nutting, 1910	CP3832-1	MNHN-IK-2009-1632	A	South-eastern slope of New Caledonia	645	–21.993	167.12	08/09/2011
I. armata Nutting, 1910	TER10084	MNHN-IK-2008-1507	B	South-eastern slope of New Caledonia	500–941	–21.996	167.105	16/10/2008
I. armata Nutting, 1910	DW3035	MNHN-IK-2008-1506		Loyalty Ridge, New Caledonia	790–800	–22.687	168.942	16/10/2008
I. armata Nutting, 1910	TER20516	MNHN-IK-2008-1510	B	Mont J, Loyalty Ridge, New Caledonia	840–800	–23.958	169.722	17/10/2008
I. armata Nutting, 1910	DW3097	MNHN-IK-2016-2540	-	South-eastern slope of New Caledonia	500–941	–22.000	167.100	26/10/2008
I. armata Nutting, 1910	DW2066	MNHN-IK-2016-2539	-	Athos Seamount, Norfolk Ridge, New Caledonia	834–870	–25.283	168.917	26/10/2008
I. armata Nutting, 1910	CP31	MNHN-IK-2011-1000	-	South-eastern slope of New Caledonia	850	–23.144	166.859	29/08/1985
I. armata Nutting, 1910 (paralectotype)	–	ZMA Coel. 02711	-	South of the western tip of Timor	520	–10.65	123.67	–
I. pseudarmata sp. nov. (paratype)	TER1021	MNHN-IK-2008-1875	C	Walpole Island, Loyalty Ridge, New Caledonia	760–820	–22.648	168.980	16/10/2008
I. pseudarmata sp. nov. (paratype)	TER1061	MNHN-IK-2008-1867	C	Walpole Island, Loyalty Ridge, New Caledonia	800	–22.678	168.965	16/10/2008
I. pseudarmata sp. nov. (paratype)	TER1062	–	A/C	Walpole Island, Loyalty Ridge, New Caledonia	800	–22.678	168.965	16/10/2008
I. pseudarmata sp. nov. (paratype)	DW3031	MNHN-IK-2008-1508	-	Walpole Island, Loyalty Ridge, New Caledonia	720	–22.646	168.975	16/10/2008
I. pseudarmata sp. nov. (paratype)	DW3036	MNHN-IK-2008-1509	-	Walpole Island, Loyalty Ridge, New Caledonia	800	–22.678	168.965	16/10/2008
I. pseudarmata sp. nov. (holotype)	DW3036	MNHN-IK-2008-1869	-	Walpole Island, Loyalty Ridge, New Caledonia	800	–22.678	168.965	16/10/2008
Isidoides sp. 1	C014597	C014597	-	East of Australia	728–826	–29.199	158.983	21/5/2003
Isidoides sp. 2	NIWA16239	NIWA 16239	A	Mahina Knoll, Bay of Plenty, New Zealand	424–534	–37.324	177.121	–
Isidoides sp. 2	NIWA41714	NIWA 41714	-	NW South Cone, Rumble III Seamount, Kermadec Ridge	700	–35.718	178.468	–

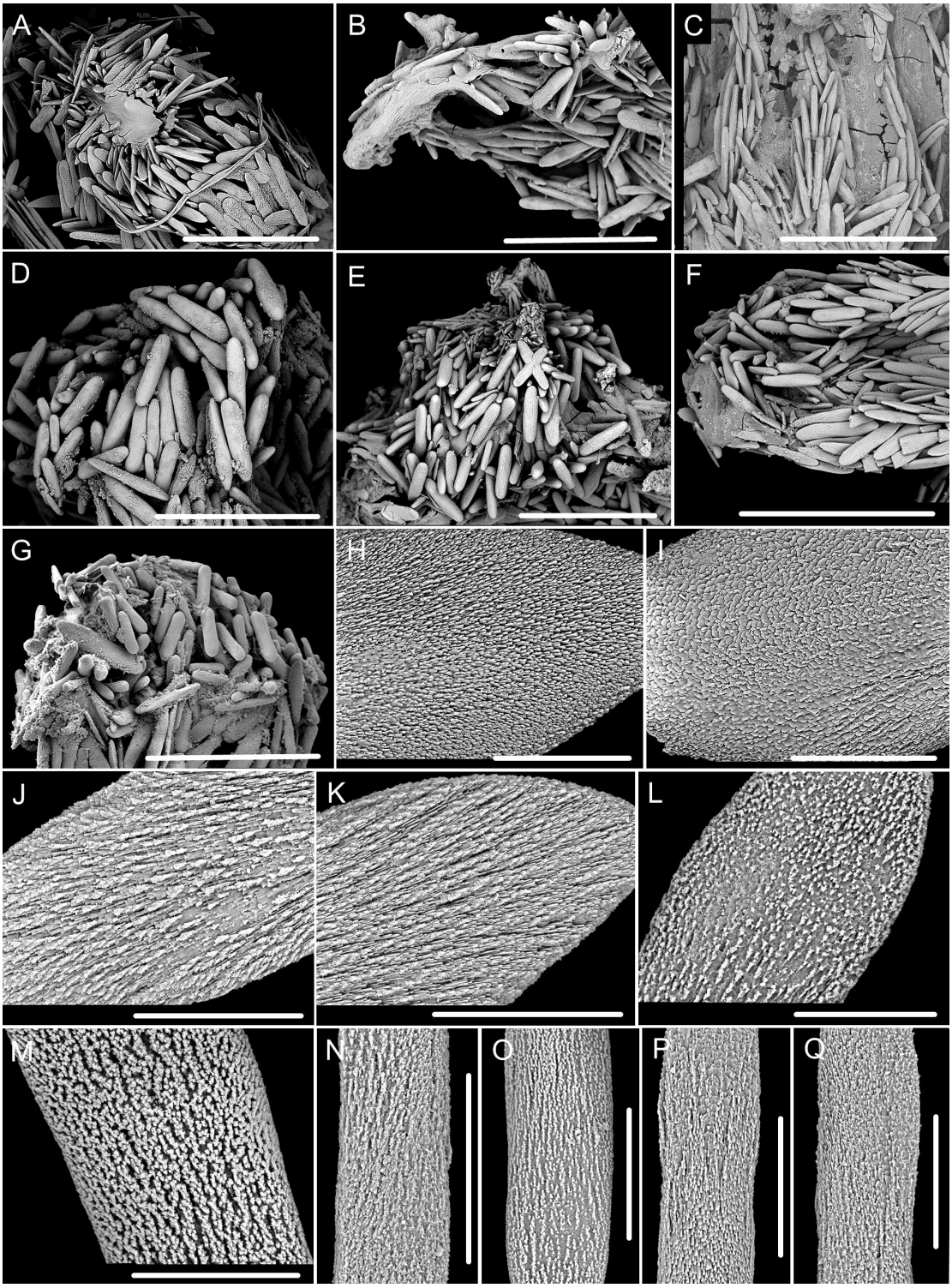

Figure 4 Morphology of tentacular sclerites (A-G), surfaces of the sclerites in the polyp body wall and coenenchyme (H-M) and in tentacles (N-O) of different *Isidoides* species. (A) flattened rods in *I. elegans* sp. nov.; (B, C) rods and flattened rods in *I. gracilis* sp. nov. (specimen Z076 and RY16141, respectively); (D) rods in *I. armata*, specimen NIWA82680; (E) rods in *I. incrassata* sp. nov.; (F) rods in *I. pseudarmata* sp. nov. (MNHN-IK-2008-1509); (G) rods in *I. armata* (paralectotype); (H) striped; (I) lamellar; (J) feather-shaped; (K) mixed shaped; (L) granulated; (M) densely granulated; (N, P, Q) non-ridged and non-granulated in *I. pseudarmata* sp. nov., *I. gracilis* sp. nov. and *I. elegans* sp. nov., respectively; (O) ridged and granulated in *I. armata*, as in *I. incrassata* sp. nov. Scale bar: 500 µm (A–G), 50 µm (H–Q)

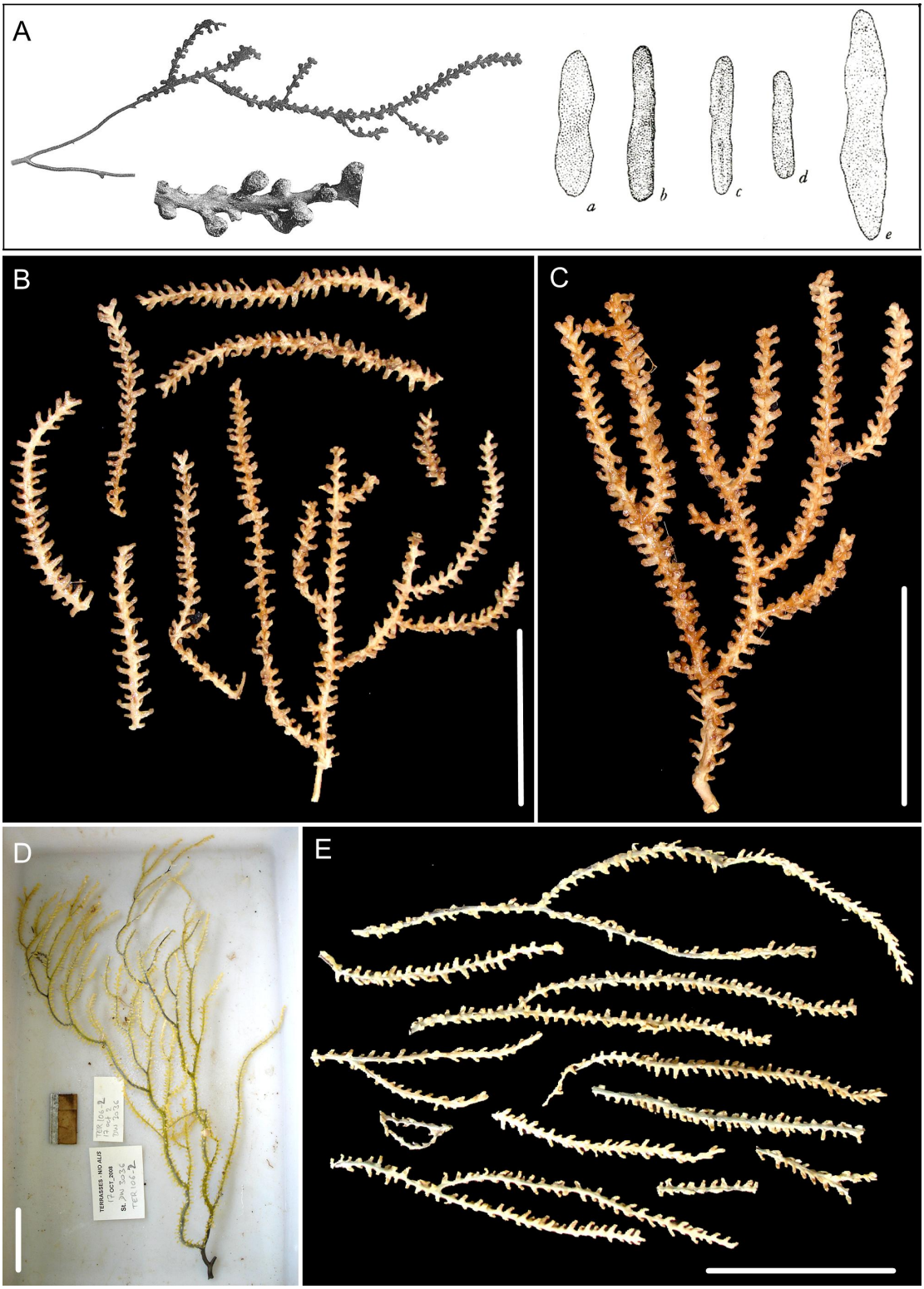

Figure 5 The lectotype of *Isidoides armata* Nutting, 1910 and some recent collections identified as "*I. armata*" by Pante et al. (2013). (A) Nutting's original illustration of *I. armata* with original figure numbering, including a large branch (15 cm long and 5 cm wide), a part of the branch with close-up of polyps and sclerites (a–e, with e being 454.5 mm tall); (B) specimen MNHN-IK-2008–1505 (TER1051) after fixation, processed from Fig. 4D in Pante et al. (2013); (C) specimen MNHN-IK-2008-1510 (TER20516) after fixation, processed from Fig. 4E in Pante et al. (2013); (D) specimen TER1062 after collection, processed from Fig. 5A in Pante et al. (2013); (E) specimen MNHN-IK-2008-1869 after fixation. Scale bar: 5 cm (B–E).

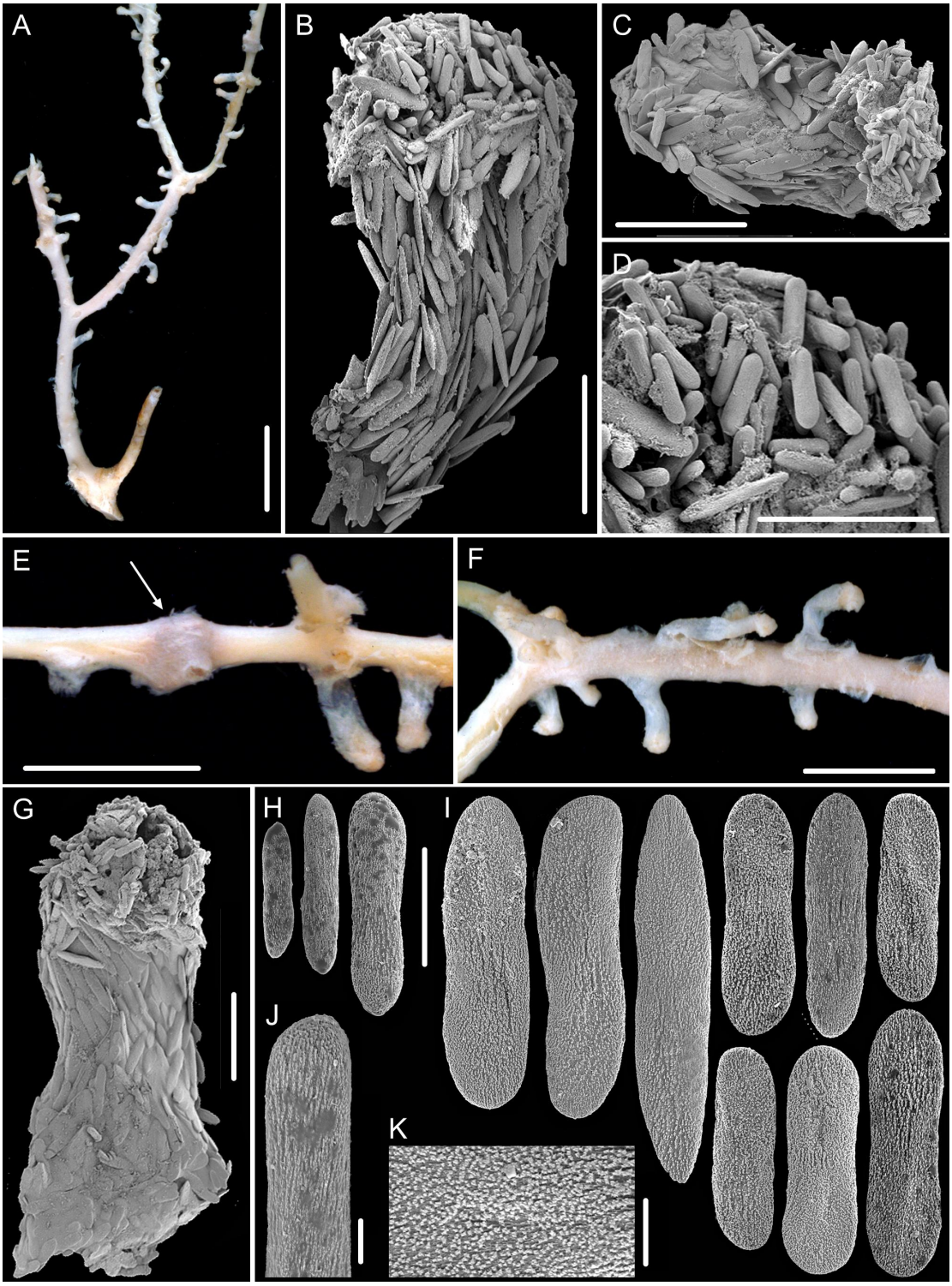

Figure 6 External morphology, polyps and sclerites of the paralectotype of *I. armata* form 2 (specimen ZMA Coel. 02711). (A) damaged fragment with few remaining polyps, with scars on the branch coenenchyme indicating that many polyps have fallen off the colony (Pante et al. 2013); (B, C, G) single polyps under SEM, among them, (B) processed from Fig. 3C in Pante et al. (2013); (E, F) part of a branch with a few polyps under a light microscope, with a feature resembling a proteinaceous node (arrow) in E, which processed from Fig. 3B in Pante et al. (2013); (H) small rods in tentacles under SEM; (I) flattened rods in polyp body wall and coenenchyme under SEM; (J) close-up of the surface of tentacle rods and polyp flattened rods under SEM, respectively. Scale bar: 1 cm (A), 5 mm (E, F), 500 µm (B, C, G), 300 µm (D), 100 µm (H and I in the same scale), 20 µm (J, K).

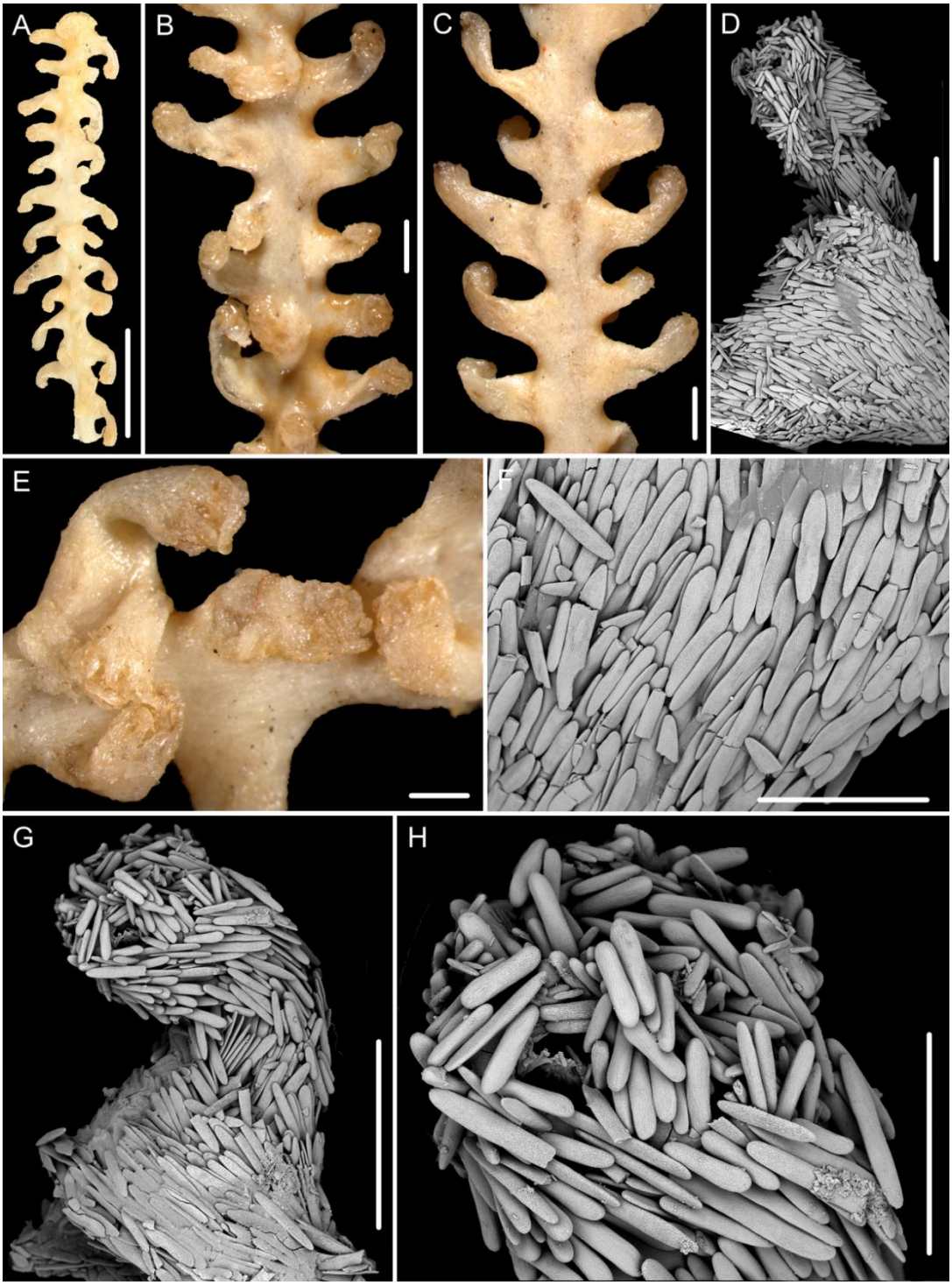

Figure 7 The external morphology and polyps of *I. armata* form 3 (specimen MNHN-IK-2008-1505). (A) separated fragment; (B, C) part of a branch under a light microscope (front and back, respectively); (D, G) polyps under SEM; (E) polyps under a light microscope; (F) basal polyp body part under SEM; (H) tentacular region under SEM. Scale bars: 1 cm (A); 2 mm (B, C); 1 mm (D, E, G), 500 μm (F, H).

Morphology of *I. armata* form 2 (paralectotype ZMA Coel. 02711, Fig. 6, based on Pante et al. 2013, present study): Axis white with semitransparent coenenchyme, white to very light brown in color. Branches irregularly pseudo-dichotomously branched (Fig. 6A). Polyps tubular with a slight bulge distally, nearly white with the head becoming very light brown after fixation, 1.2–4.7 mm in height, 0.4–1.4 mm in width (Fig. 6E, F). Polyp body wall thin and semitransparent, and polyps easily fall off the colony. Polyps

biserially distributed on two sides of branches, occasionally arranged on the front and perpendicular to the colony plane, about 1.3–4.4 mm apart. Flattened rods in polyp body wall and coenenchyme show a fine, dense, granulated appearance under SEM, longitudinally or obliquely arranged on body wall and longitudinally in coenenchyme, 0.05–0.31 mm long (Fig. 6B, C, G, I, K). Tentacles closely folded over the oral disk forming a pseudo-operculum, with small rods longitudinally arranged (Fig. 6D). These rods 0.04–0.28 mm long, the large one covered with granulated or ridged appearance, and the small one become flattened and have a non-granulated surface (Fig. 6H, J).

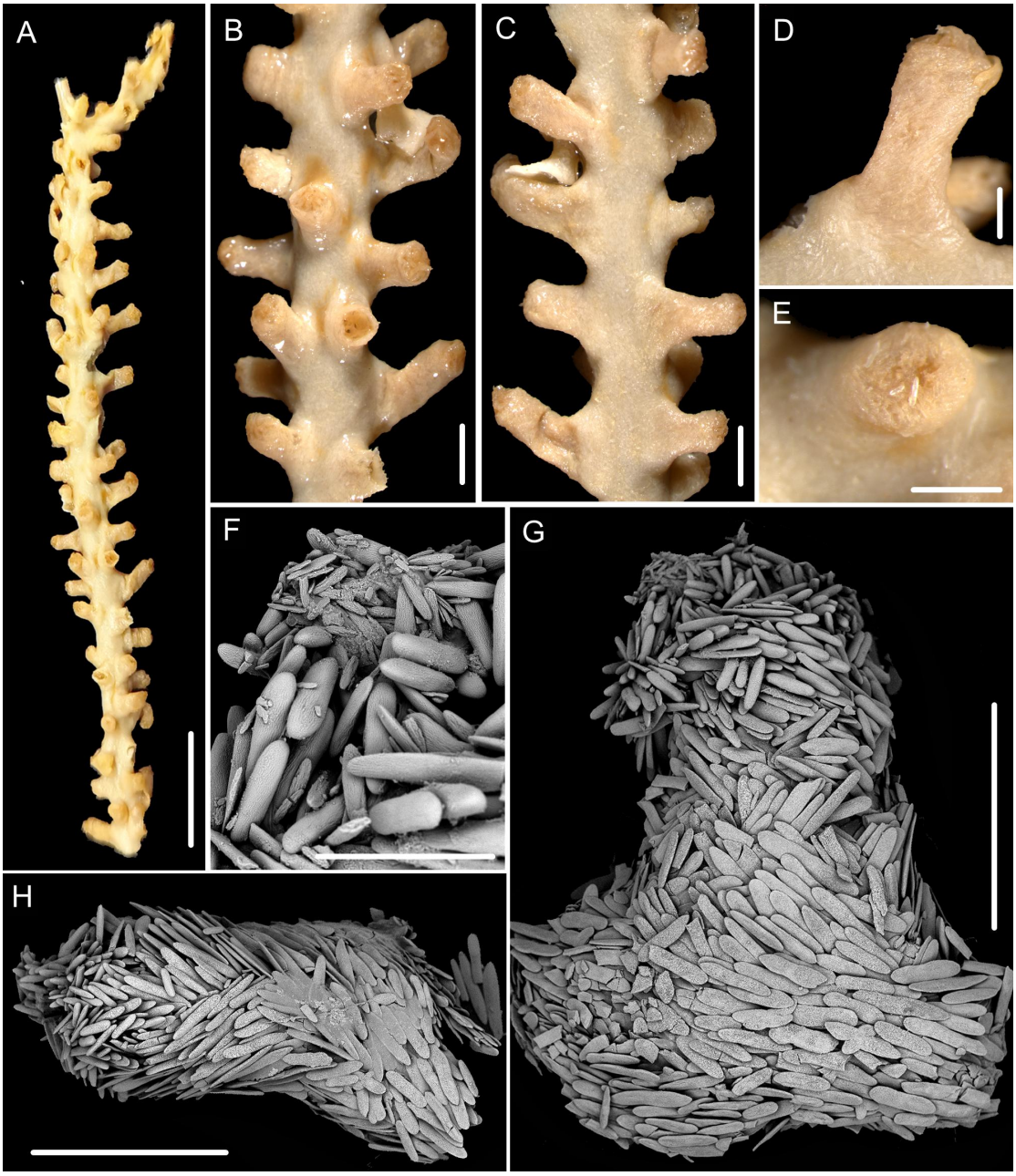

Figure 8 The external morphology and polyps of *I. armata* form 3 (specimen MNHN-IK-2009-1632). (A) separated fragment; (B, C) part of a branch under a light microscope (front and back, respectively); (D, E) polyps under a light microscope; (F) tentacular region under SEM; (G, H) single polyps under SEM. Scale bars: 1 cm (A); 2 mm (B, C); 1 mm (D, E, G, H), 300 μm (F).

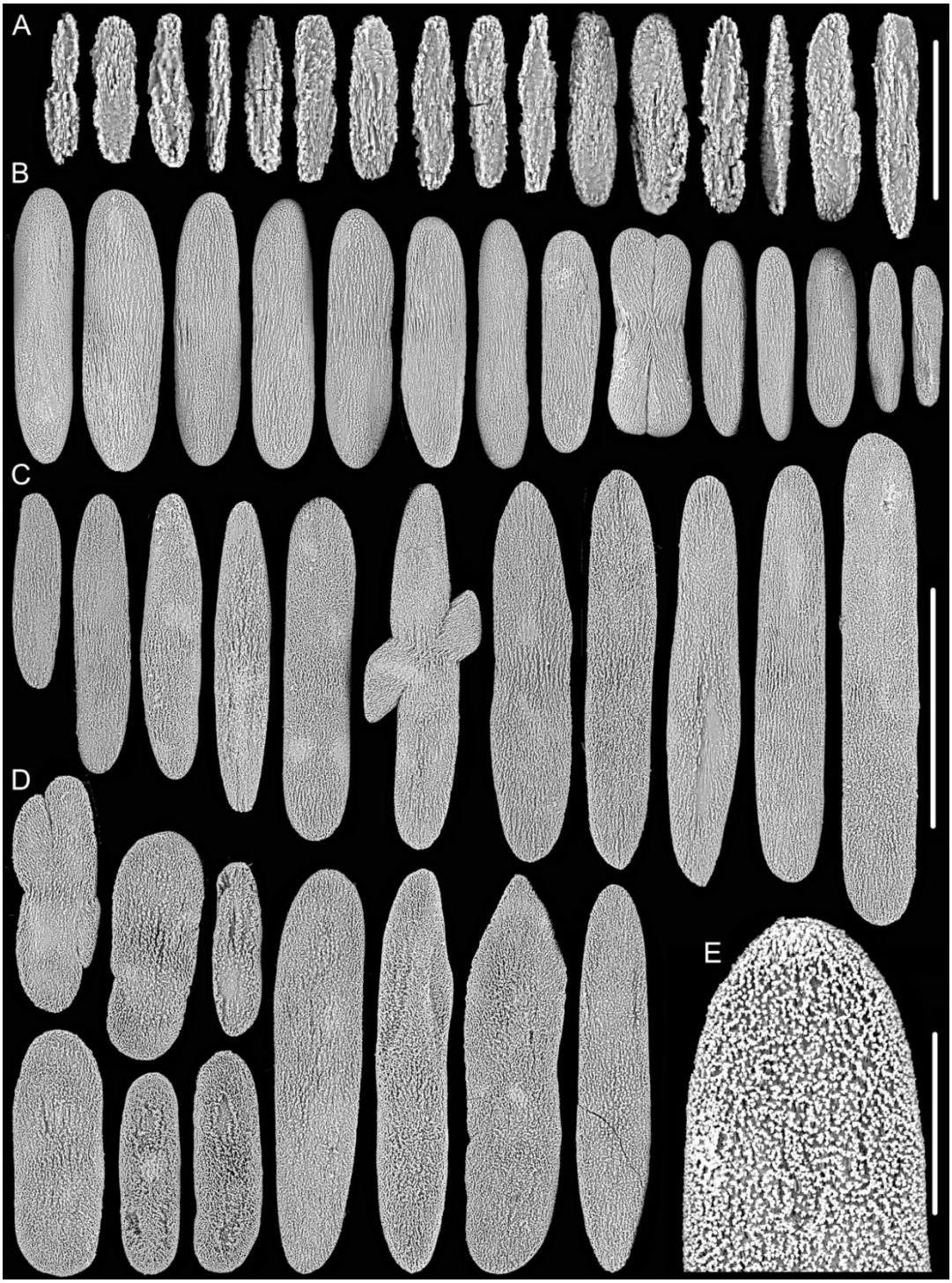

Figure 9 Sclerites of *I. armata* form 3 (specimen MNHN-IK-2009-1632). (A) small flattened rods in tentacles; (B) large rods in tentacles; (C) flattened rods in the polyp body wall; (D) flattened rods in the coenenchyme; (E) surface of sclerites. Scale bar: 200 µm (B, C, D in the same scale), 50 µm (A, E).

Morphology of *I. armata* form 3 (haplotype A and B in Pante et al. 2013: MNHN-IK-2008-1505, 2008-1411, 2008-1504, 2009-1632, 2008-1507, 2008-1506, 2008-1510, 2016-2540, 2016-2539, 2011-1000, and AMG.16995; Figs. 5B, C, 7–10; based on Pante et al. 2013, present study): Ten specimens (except AM G.16995) were re-checked. Their morphology matched well with the description in Pante et al. (2013). All of them with a cream-coloured to brown axis and cream-coloured to brown polyps after fixation. Polyps usually large, stout, and tubular with thick tissue (e.g., Figs. 7B, 8B), some of them slightly curved

and the polyp head expanded (e.g., Fig. 10C), occasionally small and conical (e.g., Fig. 9E). Polyps usually biserially arranged on two sides, sometimes with sparse polyps present on the front while absent on the back of the colony (e.g., Fig. 7B, C), occasionally irregularly arranged on all sides of branches (e.g., Fig. 10B). The surface of polyps and coenenchyme occasionally covered with abundant rice-shaped nematozooids. Sclerites all with two rounded ends (Fig. 9). Large rods in tentacle rachis with a ridged and granulated surface (Fig. 9B) while small rods become flattened with a non-granulated appearance (Fig. 9A). Flattened rods in polyp body wall and coenenchyme with a granulated appearance, sometimes become densely (Fig. 9E), some of them broad and scale-like, and with a slightly medial constriction (Fig. 9C, D).

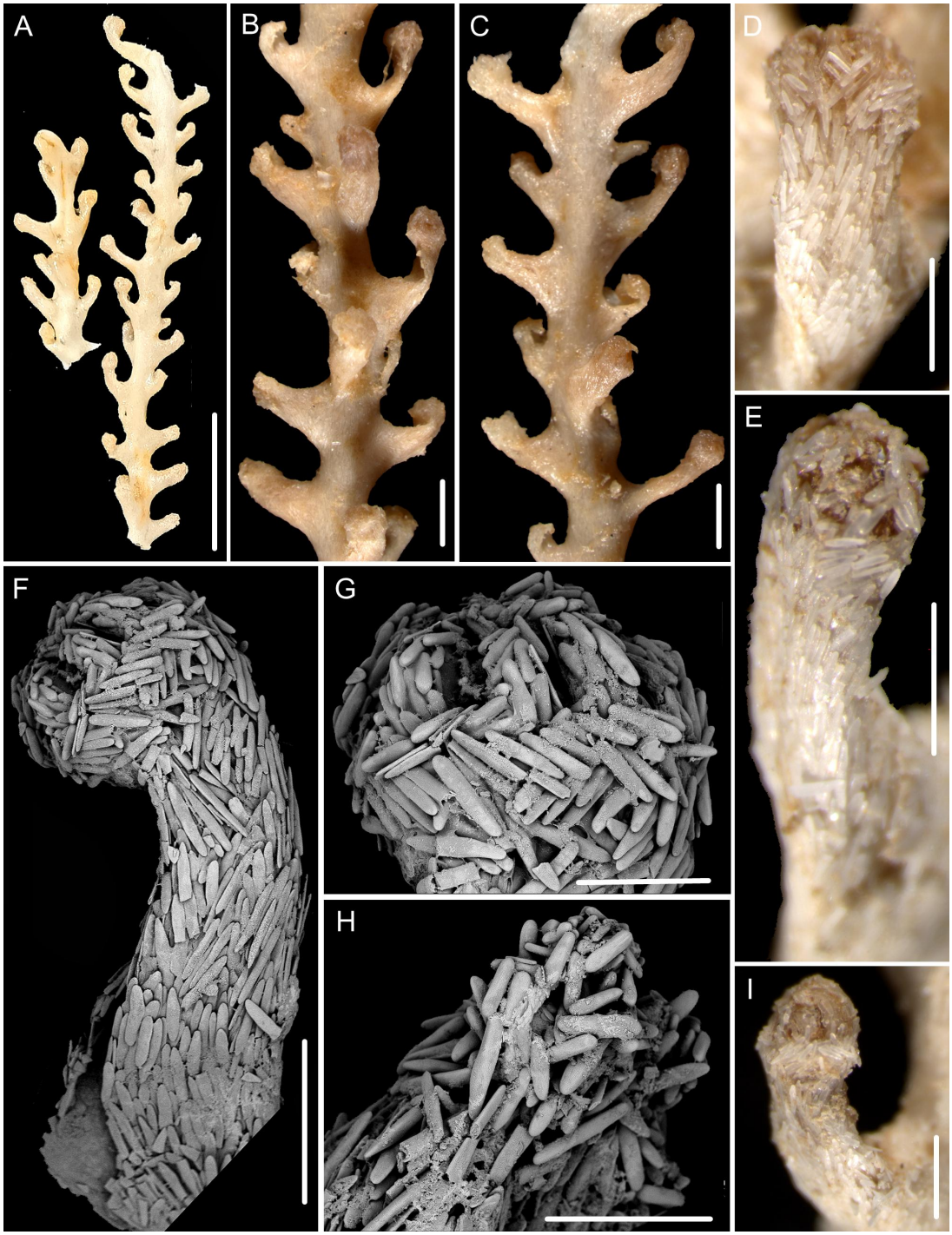

Figure 10 The external morphology and polyps of *I. armata* form 3 (specimen MNHN-IK-2016-2539). (A) the separated sample; (B, C) part of branch under a light microscope (front and back,

respectively); (D, E, I) polyps under a light microscope; (F) single polyp under SEM; (G, H) tentacular part under SEM. Scale bars: 1 cm (A); 2 mm (B, C); 1 mm (D, E, F, I), 500 µm (H), 300 µm (G).

Figure 11 The external morphology and polyps of *I. armata* form 4 (isolate MBM286881 isolated from specimen NIWA82680). (A) the specimen after fixation; (B) a part of branch under a light microscope; (C) single polyp under a light microscope; (D) polyp tentacles under SEM; (E, F) polyps under SEM. Scale bars: 2 cm (A); 2 mm (B, E, F); 1 mm (C), 500 µm (D).

Morphology of *I. armata* form 4 (NIWA 82680, Figs. 11, 12): The isolated subsample of paratype NIWA 82680, voucher isolate MBM286881 incomplete and cream-coloured (Fig. 11A). The central axis also cream-coloured, covered with a thick layer of coenenchyme. Polyps uniformly tubular with tentacles tightly folded over the oral disc, sometimes forming a slight bulge distally, but vary greatly in size, 2.0–5.5 mm long, 1.0–2.5 mm wide at base (Fig. 11B, C). Polyps usually biserially arranged on two sides of the branches, alternating between large and small forms, curved upwards, occasionally perpendicular to the colony plane between the biserial rows, 1–2 mm apart. Polyps with an opaque body wall, firmly attached to the branch and did not easily detach from the colony after fixation.

Sclerites densely arranged in polyps and coenenchyme, mostly with two rounded ends and smooth profiles, occasionally cross-shaped, some with a slightly medial constriction (Figs. 3E; 11E, F; 12). Rods in the back of the tentacle rachis longitudinally arranged, the large ones having a ridged and granulated appearance, while the small ones usually non-granulated, measuring 50–332 × 10–63 µm (Figs. 4O; 11D; 12A, B). Flattened rods in the polyp body wall longitudinally or obliquely arranged, measuring 183–466 × 25–78 µm (Figs. 11E, F; 12C). Sclerite forms in the coenenchyme same as in the polyp body wall, arranged along the branch, some of them broad and scale-like, and measuring 150–412 × 40–119 µm (Fig. 12D).

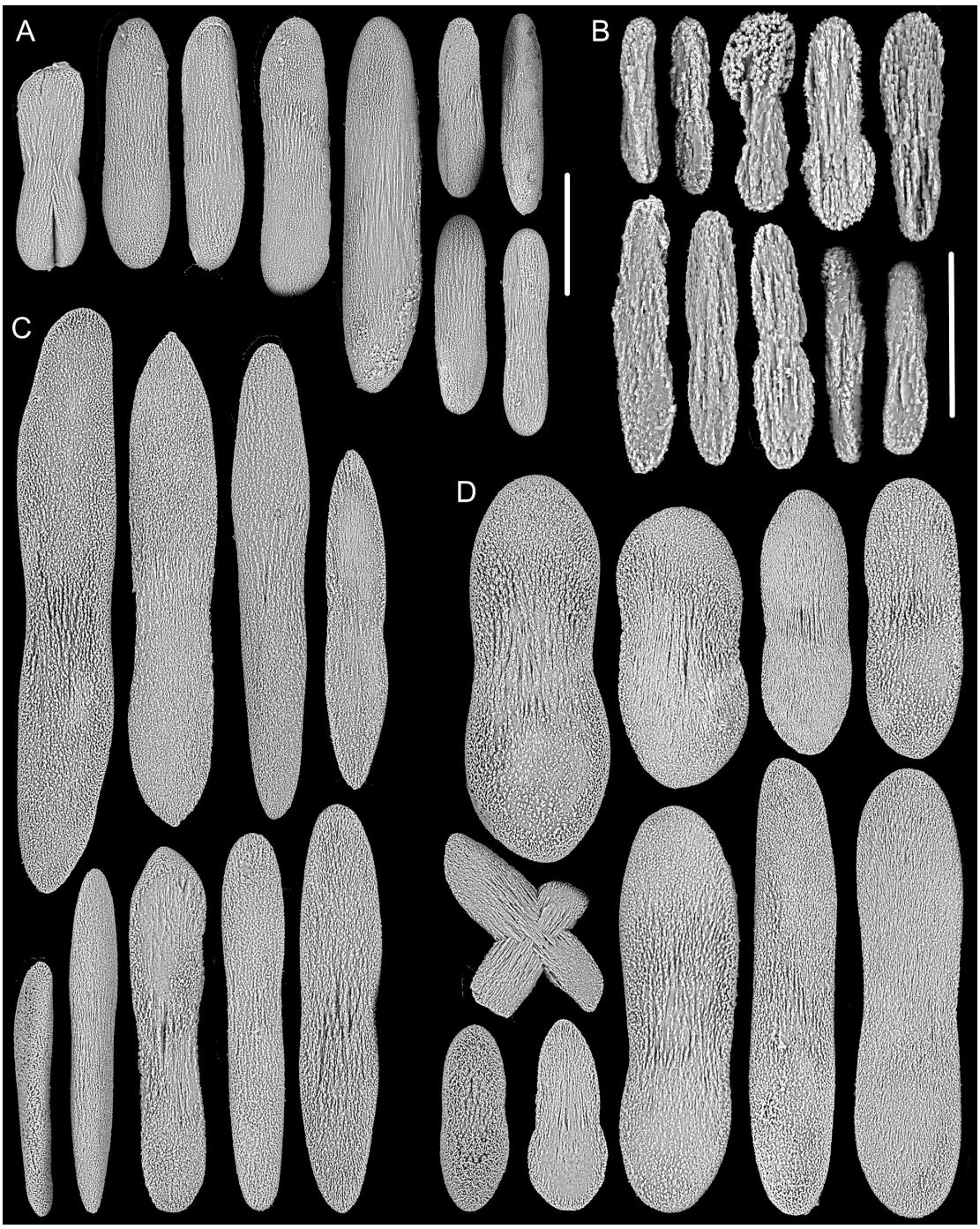

Figure 12 Sclerites of *I. armata* form 4 (isolate MBM286881 isolated from specimen NIWA82680). (A) large sclerites in tentacles; (B) small sclerites in tentacles; (C) sclerites in the polyp body wall; (D) sclerites in coenenchyme. Scale bar: 100 µm (A, C, D in the same scale), 50 µm (B).

Type locality. 10.65°S, 123.67°1E, south of the western tip of Timor, 520 m (Pante et al., 2013).

Distribution. 5.9°S, 132.945°E, eastern slope of Elat, Kei Islands, Arafura Sea, 984 m (Nutting, 1910); 10.65°S, 123.67°1E, south of the western tip of Timor, 520 m (Pante et al., 2013); New Caledonia to New Zealand, including south-eastern slope of New Caledonia, Norfolk Ridge, Loyalty Ridge, Kermadec Ridge and Bay of Plenty, 500–1065 m (Table 5, Pante et al., 2013, present study).

Remarks. The four forms of *I. armata* all have pseudo-dichotomous and irregular branching, light-coloured of axis, and the same sclerite forms, including large rods with a ridged and granulated appearance in the tentacle rachis and flattened rods with a granulated appearance in the polyp body wall and coenenchyme. Nonetheless, obvious morphological variations were observed in colony color, polyp shape, thickness, and arrangement (Table 5),. However, these differences were not constant and were possibly caused by different growth stages or environments. Given that the sclerite forms are stable and reliable for octocoral species identification (e.g., Xu et al., 2021a), we identified the four forms as the same species.

The morphological identification was also supported by the phylogenetic analysis of Sanger and UCE sequencing data, which showed that *I. armata* forms 3 and 4 are within the intraspecific differences (see the genetic analysis aforementioned). The haplotypes A and B defined by Pante et al. (2013) were identified as the form 3, while the haplotype C is described as a new species, as described below.

***Isidoides incrassata* Xu, Bilewitch & Pante sp. nov.**

Figs. 4E, M; 13, 14

urn:lsid:zoobank.org:act:E2455474-7733-4AD4-AED7-1DBB8A2FB5F2

Holotype: NIWA163516, NIWA stn Z9224, 37.1°S, 177.3°E, collected from the Bay of Plenty, New Zealand, 614 m, 13 August 1998. Other material: MBM286882, voucher isolate from the holotype.

Diagnosis: Colony deep ochre with a light brown central axis and a thick layer of coenenchyme. Polyps conical and tubular, densely arranged on all sides of the branches. Tentacles tightly folded over the polyp heads. Rods and flattened rods with densely granulated surface in polyp body wall and coenenchyme, rods with ridged surface in tentacles.

Description: Holotype incomplete and planar, with deep ochre color after fixation and the holdfast not recovered, about 22 cm in height (Fig. 13A). The central axis light brown, covered with a thick layer of coenenchyme. Branches irregularly and pseudo-dichotomously branched in one plane, with the terminal branchlets up to 6 cm long (Fig. 13A). Polyps conical and tubular with a uniform size, 2–3 mm long, 1–2 mm wide, densely arranged on all sides of the branches (Fig. 13B, F). Polyps with an opaque and thick body wall, firmly attached to the branch, and did not easily detach from the colony after fixation. Tentacles indistinct and tightly folded over the polyp heads, the basal part of tentacles sometimes contracting to form a operculum-like structure. The surface of polyps and coenenchyme often covered with abundant rice-shaped nematozooids, measuring 10–20 μm in length (Fig. 13D, E).

Sclerites densely arranged in polyps and coenenchyme, with two rounded ends and mostly smooth profiles, occasionally cross-shaped and with large warts (Figs. 13G, 14). Rods in the back of tentacle rachis longitudinally arranged, covered with a ridged and granulated appearance, and measuring 35–220 × 9–48 μm (Figs. 13C, G; 14A, B). Rods in the polyp body wall almost flattened, longitudinally or obliquely arranged, covered with a very densely granulated appearance, measuring 56–440 × 17–72 μm (Fig. 14C, E). Sclerite forms in coenenchyme same as in the polyp body wall, arranged along the branch, but relatively large, occasionally with large warts, and measuring 84–508 × 27–128 μm (Fig. 14D).

Type locality: Bay of Plenty in New Zealand, 614 m.

Etymology: The Latin adjective *incrassatus* (incrassate) refers to the thick coenenchyme of this species.

Distribution: Found from the Bay of Plenty in New Zealand at a water depth of 614 m.

Remarks: *Isidoides incrassata* sp. nov. is characterized by a deep ochre color, conical or tubular polyps densely distributed on the branches, and slender and flattened rods in polyp body wall and coenenchyme all with densely granulated surface. The new species is similar to *I. armata* in having certain granulated sclerites, but differs in the size and shape of polyps (conical and tubular, up to 3.0 mm long? *vs.* uniformly wart-like/bud-like or tubular often with enlarged distal ends, up to 6 mm). In addition, the new species has a deep ochre color after ethanol fixation and the sclerites are mostly elongate elliptical, while *I.*

armata is light brown with sclerites that are usually constricted in the middle portion (Table 5).

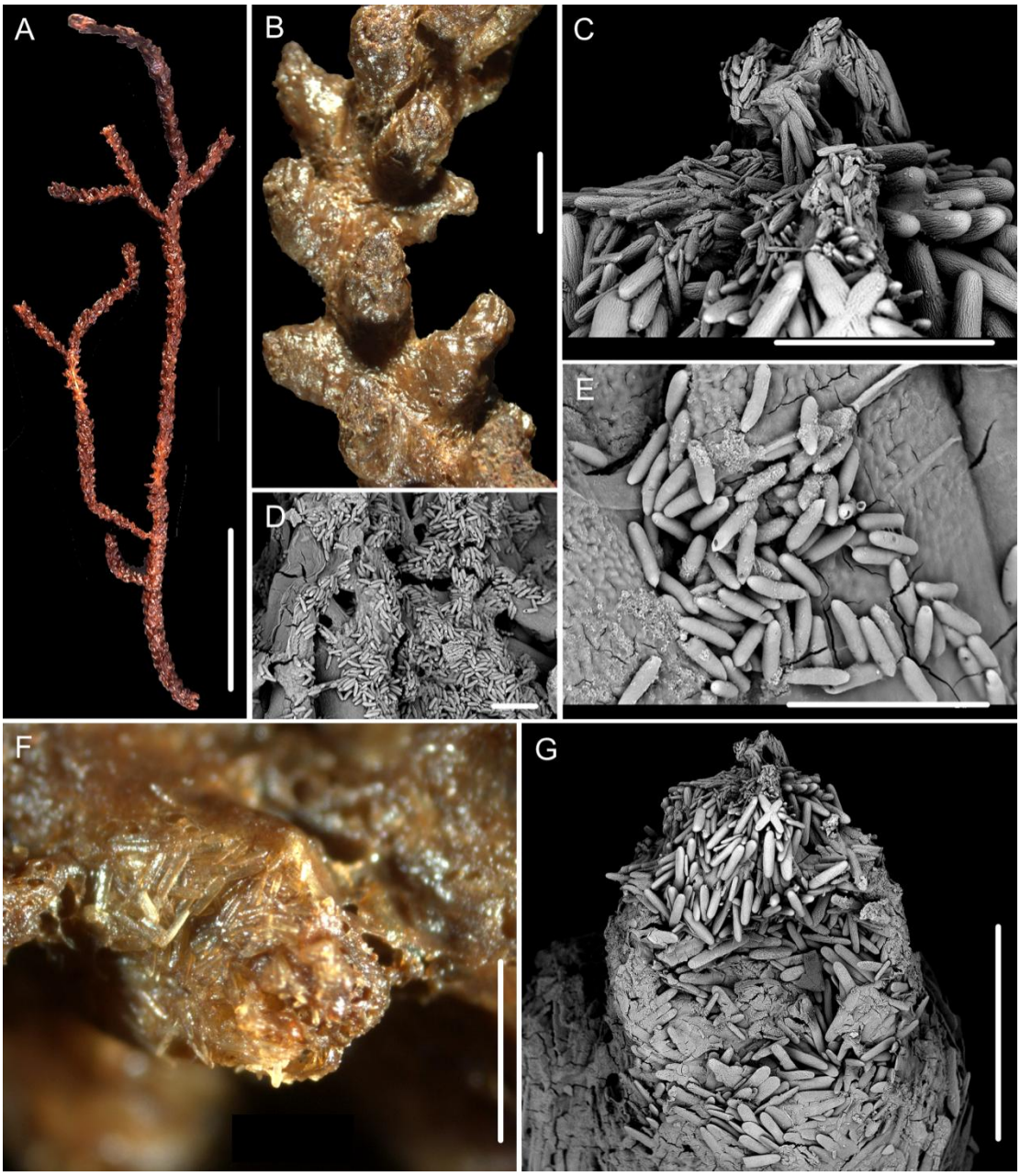

Figure 13 External morphology and polyps of *Isidoides incrassata* sp. nov. (A) holotype after fixation; (B) part of branch under a light microscope; (C) tentacular part under SEM; (D, E) nematozooids on the surface of polyps and coenenchyme under SEM; (F, G) single polyp under a light microscope and SEM. Scale bars: 5 cm (A); 2 mm (B); 1 mm (F, G); 300 µm (C); 50 µm (D, E).

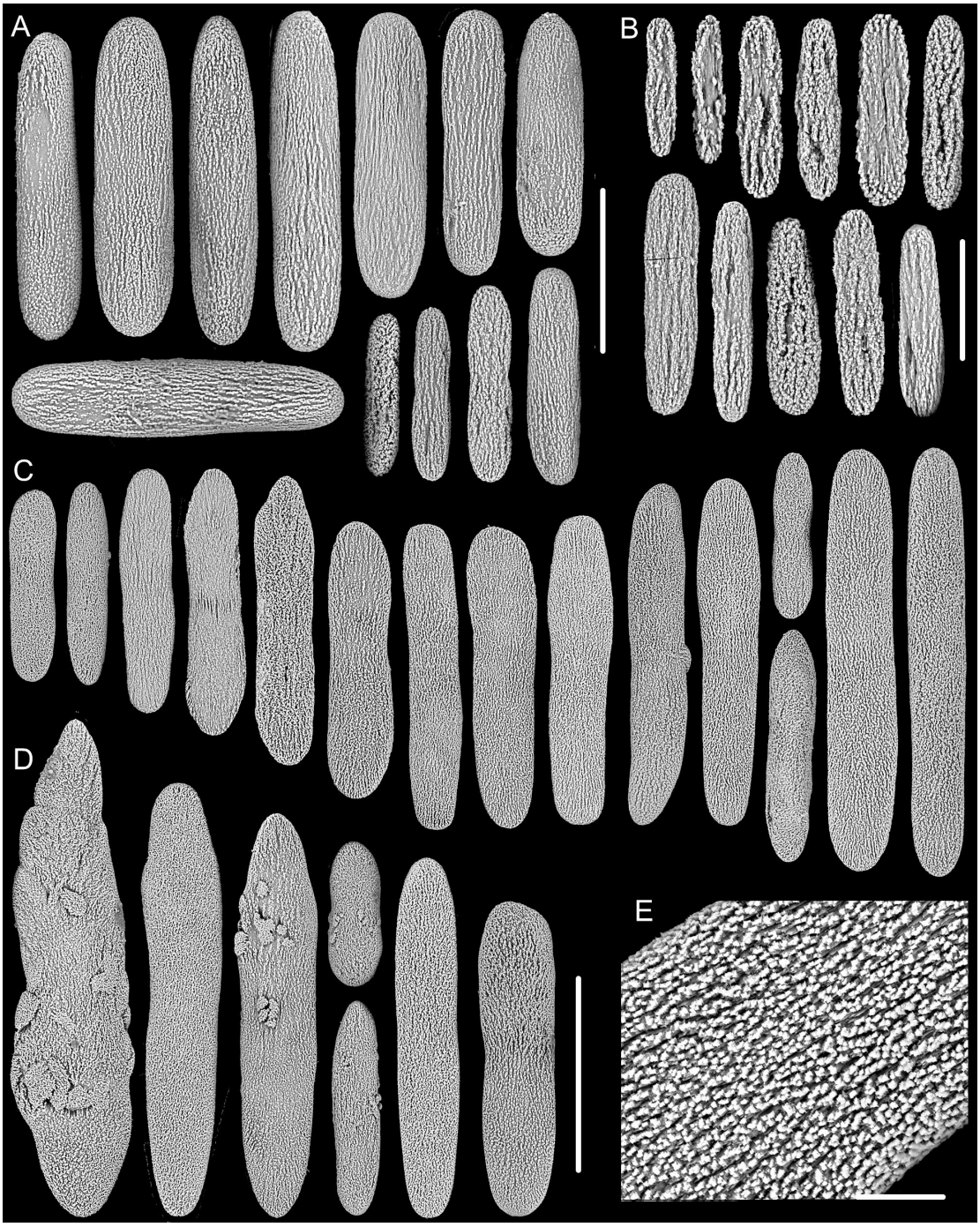

Fig. 14 Sclerites of *Isidoides incrassata* sp. nov. (A) large sclerites in tentacles; (B) small sclerites in tentacles; (C) sclerites in the polyp body wall; (D) sclerites in coenenchyme; (E) surface of the sclerites. Scale bar: 200 µm (C, D in the same scale), 100 µm (A), 50 µm (B), 20 µm (E).

Isidoides pseudarmata **Xu, Bilewitch & Pante sp. nov.**
Figs. 4F, N; 5D, E; 15–17
urn:lsid:zoobank.org:act:729D9319-A9A8-4E51-AE8E-65B7E3660501

Material examined: Holotype: MNHN-IK-2008-1869; **Paratypes:** MNHN-IK-2008-1875 (TER1021), 2008-1867 (TER1061), 2008-1508, 2008-1509 and specimen TER1062 in Muséum national d'Histoire naturelle in Paris, France. The collection information of these specimens listed in Table 5.

482 **Table 5** Morphological features and comparisons among the Isidoides species. "–" means unknown data.

Characters/Species	*I. armata* Nutting 1910				*I. incrassata* sp. nov.
	form 1 (lectotype)	form 2 (paralectotype)	form 3 (e.g., MNHN-IK-2008-1505)	form 4 (NIWA82680)	
Sample size	1	1	10	1	1
Colony color in life /after fixation	–/ very light brown	–/ white to very light brown	–/cream-coloured to brown	–/cream-coloured	–/deep ochre
Axis color	very light brown	white	cream-coloured to light brown	cream-coloured	light brown
Branching pattern	irregularly pseudo-dichotomous	irregularly pseudo-dichotomous	irregularly pseudo-dichotomous	–	irregularly pseudo-dichotomous
Inter-polyps distance (mm)	–	1.3–4.4	up to 4.8	1.0-2.0	–
Polyp shape	tubular or club-shaped, the polyp head always expanded (wart-like or bud-like)	soft tubular, the polyp head sometimes expanded	small conical and large stout tubular, sometimes slightly curved and the polyp head expanded	large slender tubular, sometimes slightly curved and the polyp head expanded	small conical and tubular
Status of polyps body wall at base	opaque, and contracted	translucent, and not contracted	opaque, and not contracted	opaque, and not contracted	opaque, and not contracted
Polyp height/width when contracted (mm)	mostly 1.8, up to 4.0/ 1.4–1.5	1.2–4.7/ 0.4–1.4	1.0–5.9, most more than 2/ 0.4–3.0	2.0–5.5/1.0–2.5	2.0–3.0/1.0–2.0
Polyp arrangement	biserially arranged, sometimes irregularly on all sides of distal branchlets	biserially arranged, occasionally on the front	biserially arranged on two sides, sometimes on the front and absent on the back, occasionally irregularly arranged on all sides	biserially arranged, occasionally on the front	irregularly and densely arranged on all sides
Sclerites in tentacles with maximum length (mm)	bar-like/ –	rods/ 0.28	rods/ 0.41	rods/ 0.33	rods/ 0.22
Sclerite surface of large rods in tentacle	dense granulated	ridged and granulated	ridged and granulated	ridged and granulated	ridged and granulated
Sclerites in polyp body and coenenchyme with maximum length (mm)	all with two rounded ends and often with a slightly medial constriction/ 0.45	almost with two rounded ends, sometimes broad, and scale-like, and with a slightly medial constriction/ 0.31	almost with two rounded ends, sometimes broad, and scale-like, and with a slightly medial constriction/ 0.50	almost with two rounded ends and a slightly medial constriction, sometimes broad and scale-like/ 0.47	slender with two rounded ends/ 0.51
Sclerites surface of polyp body and coenenchyme	densely granulated	granulated, sometimes densely	granulated, sometimes densely	granulated, occasionally densely	densely granulated
Distribution	Kei Islands, Arafura Sea	south of the western tip of Timor	New Caledonia to New Zealand	Bay of Plenty, New Zealand	Bay of Plenty, New Zealand
Depth (m)	984	520	614–1065	878	614
Figures	5A	6	5B, C; 7–10	11, 12	13, 14

483

Continued.

Characters/Species	*I. elegans* sp. nov.	*I. gracilis* sp. nov.		*I. pesudarmata* sp. nov.
		form 1 (e.g., MBM286877)	form 2 (MBM286880)	
Sample size	2	3	1	5
Colony color in life /after fixation	deep brown to ochre/ deep brown to ochre	yellow/ light to deep brown	–/ gray to brown	yellow/ very light brown
Axis color	off-white	brown to nearly black	gray	dark golden-brown to black
Branching pattern	irregularly pseudo-dichotomous	irregularly pseudo-dichotomous	irregularly pseudo-dichotomous	branches traced a distinct upward curve to eventually follow (more-or-less) the direction of the parent branch, forming a nearly lyrate pattern
Inter-polyps distance (mm)	up to 3.0	up to 2.0	up to 1.0	up to 1.5
Polyp shape	large stout tubular and small wart-like/ bud-like, the polyp head sometimes expanded	large soft tubular with extended tentacles, and small wart-like/dome-shaped	large soft tubular with extended tentacles	small conical and slender tubular, sometimes curved, the polyp head often expanded
Status of polyps body wall at base	opaque, and partially contracted	opaque, and not contracted	opaque, and not contracted	opaque, and not contracted
Polyp height/width when contracted (mm)	0.5–6.0/ 1.0–2.5	0.5–3.5/ 1.0–1.5	1.0–6.0/ 1.0–1.5	0.5–4.0/ 0.5–1.5
Polyp arrangement	biserially arranged, sometimes irregularly on all sides of distal twigs	irregularly and densely arranged, sometimes biserially on terminal branchlets	biserially arranged	biserially and nearly alternately arranged
Sclerites in tentacles with maximum length (mm)	flattened rods/ 0.28	almost flattened rods/ 0.26	flattened rods/ 0.19	rods/ 0.25
Sclerite surface of large rods in tentacle	non-ridged and non-granulated	almost non-ridged and non-granulated, occasionally granulated in small one	non-ridged and non-granulated	non-ridged and non-granulated
Sclerites in polyp body and coenenchyme with maximum length (mm)	slender, often spindle-like, sometimes with a slightly medial constriction/ 0.64	often with two rounded ends and a slightly medial constriction, sometimes with large warts/ 0.49	often with two rounded ends and a slightly medial constriction, the outline relatively irregular/ 0.44	slender, often spindle-like/ 0.59
Sclerites surface of polyp body and coenenchyme	non-granulated	almost non-granulated, occasionally sparsely granulated	almost non-granulated, occasionally sparsely granulated	densely granulated
Distribution	a seamount on the Caroline Ridge	South China Sea	South China Sea	Loyalty Ridge, New Caledonia
Depth (m)	814–962	586–910	811 m	760–820
Figures	18–20	21–24, 25A, C, E; 26D	25B, D; 26A–C, E–G; 27	5D, E; 15–17

Diagnosis: Colony planar and yellow when alive but became very light brown after fixation. Axis dark golden-brown to black. Branches traced a distinct upward curve to eventually follow (more-or-less) the direction of the parent branch, forming a nearly lyrate pattern. Polyps slender and tubular with the head often swollen, occasionally small and conical, usually biserial, alternating between large and small forms, obliquely towards to the distal end. Rods in tentacles with a non-granulated appearance. Flattened rods in polyps and coenenchyme slender, often spindle-like with a densely granulated appearance.

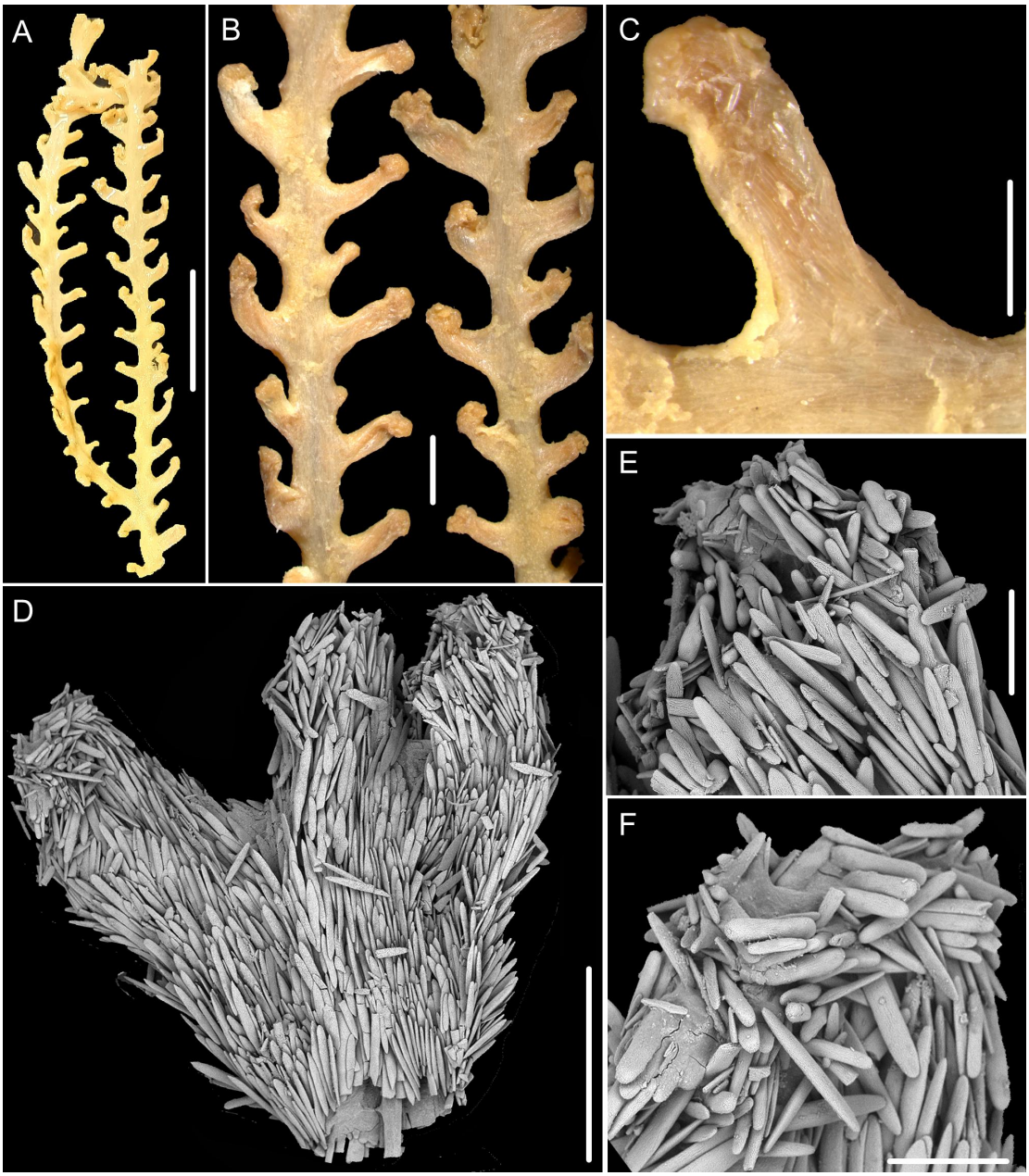

Figure 15 The external morphology and polyps of specimen MNHN-IK-2008-1869. (A) the separated sample; (B, C) two parts of branch under a light microscope; (C) single polyp under a light microscope; (D) two polyps under SEM; (E, F) tentacular part under SEM. Scale bars: 1 cm (A), 2 mm (B); 1 mm (C, D), 200 µm (E, F).

Description: Specimen of holotype MNHN-IK-2008-1869 incomplete and broken with missing holdfast , very light brown after fixation (Fig. 5E). While the specimen TER1062 yellow and planar with the branches traced a distinct upward curve to eventually follow (more-or-less) the direction of the parent branch, forming a nearly lyrate pattern based on the picture after collection (Fig. 5D). The colony covered with a relatively thin layer of coenenchyme and a dark golden-brown to black axis. Polyps 0.5–4.0 mm

long, 1.0–1.5 mm but mostly 1.0 mm wide, slender and tubular with the head often expanded, sometimes curved, occasionally small and conical, firmly attached to the branch and not easily fallen off the colony after fixation (e.g., Fig. 15B, C). Polyps usually biserial and alternating between large and small forms, obliquely towards to the distal, up to 1.5 mm apart.

Figure 16 The external morphology and polyps of specimen MNHN-IK-2008-1875. (A) the separated sample; (B) two parts of branch under a light microscope; (C) tentacular part under SEM; (D) coenenchymal sclerites under SEM; (E) two polyps under SEM; (F) two polyps under a light microscope. Scale bars: 1 cm (A), 2 mm (B); 1 mm (E, F), 500 µm (D), 300 µm (C).

Sclerites densely arranged in polyps and coenenchyme, occasionally crossed-shaped (Figs. 15D, 17). Rods in the back of the tentacle rachis with two rounded ends and a non-granulated appearance, occasionally flattened, and measuring 63–250 × 11–62 µm (Figs. 4N; 15E, F; 17A, B). Flattened rods in

polyp body walls and coenenchyme slender, often spindle-like with a densely granulated appearance, some of them with two rounded ends, longitudinally or obliquely arranged, measuring 123–397 × 31–59 μm (Fig. 17B) and 143–590 × 25–103 μm (Fig. 17C), respectively.

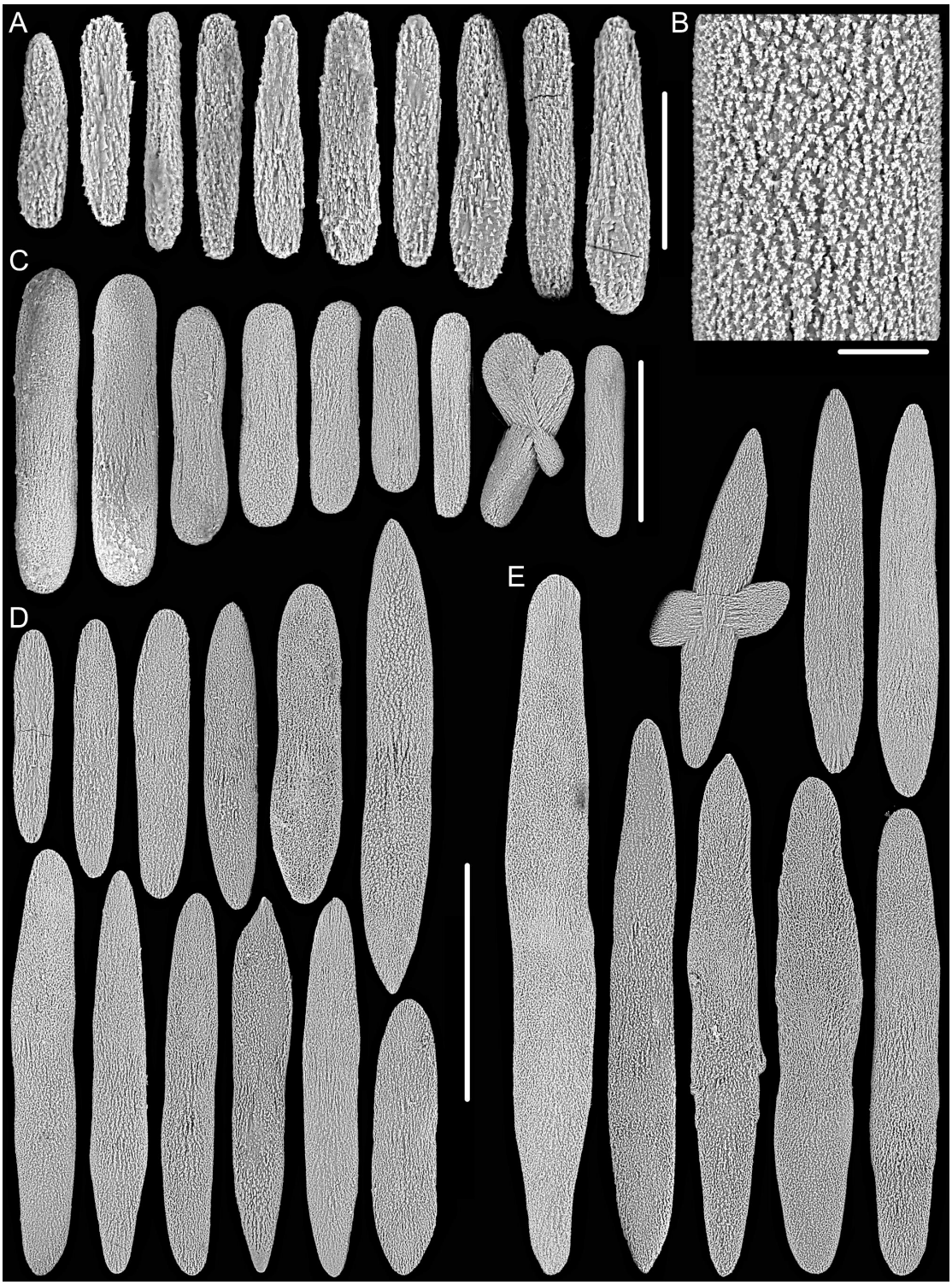

Figure 17 Sclerites of specimen MNHN-IK-2008-1869. (A) small sclerites in tentacles; (B) surface of the sclerites; (C) large sclerites in tentacles; (D) sclerites in the polyp body wall; (E) sclerites in coenenchyme. Scale bar: 200 μm (D, E in the same scale), 100 μm C), 50 μm (A), 20 μm (B).

Variability of paratype: The polyps of three specimens of paratype are relatively small, among them,

MNHN-IK-2008-1867 up to 2.5 mm, 2008-1875 and 2008-1509 up to 3.0 mm.

Type locality: Walpole Island, Loyalty Ridge, New Caledonia, 800 m.

Etymology: Composition of the Greek prefix pseud- (fake) and the species name *armata*, referring to the similarity of the new species with *I. armata*.

Distribution: New Caledonia with water depths of 760–820 m.

Remarks: The examined specimens were previously defined as haplotype C of *I. armata* (Pante et al., 2013). Based on the examination of five specimens and the phylogenetic analysis in this study, we separated these specimens from *I. armata* and establish a new species. *Isidoides pseudarmata* sp. nov. differs from *I. armata* by having a dark golden-brown to black axis (vs. white to light brown), relatively slender and small polyps with thin tissue (vs. usually stout and large with thick tissue), large rods in tentacles with a non-granulated appearance (vs. granulated or ridged), and slender and often spindle-like sclerites (vs. relatively broad, sometimes scale-like with a slightly medial constriction) in the polyp body and coenenchyme (Table 5).

***Isidoides elegans* Xu, Bilewitch & Pante sp. nov.**

Figs. 4A, Q; 18–20

urn:lsid:zoobank.org:act:02A4B99F-01BC-45E8-97F3-61AF1DD01AAE

Material examined: Holotype: MBM286500, station FX-Dive 213 (10°04.60′N, 140°11.40′E), an unnamed seamount located on the Caroline Ridge, 814 m, 31 May 2019. **Paratype:** MBM286501, station FX-Dive 209 (10°04.68′N, 140°12.17′E), the same seamount on the Caroline Ridge, 962 m, 27 May 2019.

Diagnosis: Colony planar, deep brown to ochre color after fixation with an off-white central axis. Polyps vary greatly in size and shape, including large and tubular or small and wart-like, usually biserial, alternating between large and small forms, and occasionally present on all sides of the distal twigs. Tentacles tightly folded into the hollow oral disc or gathered at the head of the polyps. Sclerites all flattened and thin rods with a non-granulated surface, usually slender and spindle-like and with a slightly medial constriction.

Description: Holotype planar with a deep brown to ochre color in life, about 27 cm in height and 50 cm in maximum width (Fig. 18A, B). Holdfast calcareous and nearly oval, about 35 mm in maximal length and 22 mm in width, attached firmly to rock. The main stem below the first branch short, about 3 mm long and 4 mm in diameter at the base. The central axis solid and off-white, covered with a thick layer of coenenchyme, occasionally a calcareous but not horny bulge present on the branch axis. Branches irregularly and pseudo-dichotomously branched in one plane, and nearly parallel to the adjacent branches (Fig. 18B, C). Anastomosis of branches never observed. Distance between adjacent branches 0.5–6.5 cm, and the terminal branchlets up to 31 cm long and 0.6–2.0 mm wide.

Polyps varied greatly in size and shape, including large tubular, and small wart-like/bud-like forms (similar to the polyps shape of lectotype of *I. armata* and *Iridogorgia densispicula* Xu, Zhan, Li & Xu, 2020, fig. 2C, D in Xu et al. 2020), with distal ends always enlarged (Fig. 19). Polyps usually biserially arranged on each side of axis, alternating between large and small forms, and occasionally present on all sides of the distal twigs (Fig. 19A). Sometimes polyps all large tubular or all small wart-like on the branchlets (Fig. 19B, C). Polyps almost parallel to the colony plane, some of them curved in different directions, occasionally perpendicular to the colony plane (Fig. 19A–C). Polyps 0.5–6.0 mm long, 0.5–2.5 mm wide, and 0.1 to 3.0 mm apart. Polyps with an opaque and thick body wall, firmly attached to the branch and not easily fallen off the colony after fixation. Tentacles contractile and tightly folded into the hollow oral disc or gathered at the head of the polyps (Fig. 19D, E).

Polyps and coenenchyme covered with dense sclerites and a deep brown to ochre layer of cortex on the surface, and the color unchanged after fixation in ethanol (Fig. 19A–C). Sclerites are flattened and thin rods, some with a slightly medial constriction, occasionally crossed-shaped (Fig. 20). Their surfaces non-granulated, usually striped, feather-shaped or of mixed shapes, and rarely lamellar (Fig. 4H–K). Sclerites in the back of the tentacle rachis longitudinally arranged, slender with two rounded ends, measuring 63–278 × 11–50 μm (Fig. 20A, B). Sclerites in the polyp body wall longitudinally or obliquely arranged, some transversely arranged or crosswise on the upper margin. They often had a slightly medial constriction and sometimes spindle-like with two pointed ends, measuring 94–643 × 25–140 μm (Fig. 20C). Sclerite forms

in the coenenchyme same as in the polyp body wall, arranged along the branch, measuring 136–615 × 32–120 μm (Fig. 20D).

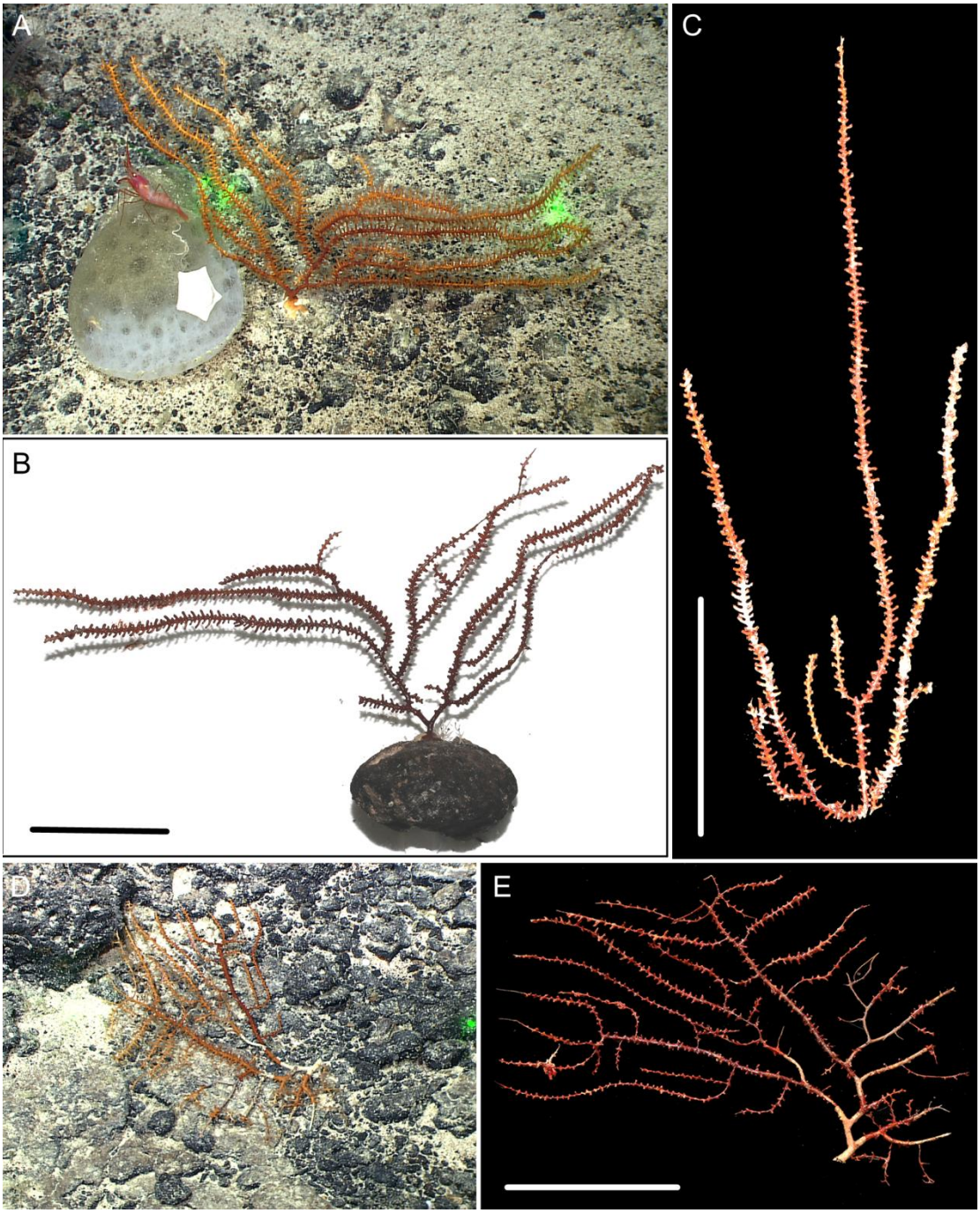

Figure 18 External morphology of *Isidoides elegans* sp. nov. (A, B) holotype *in situ* and after collection; (C) a broken branch of holotype; (D, E) paratype *in situ* and after collection. Scale bars: 10 cm (B, E), 5 cm (C).

Variability of paratype: Paratype planar with holdfast absent when it was discovered, about 15 cm high and 25 cm wide (Fig. 18D, E). The basal stem and some branches bare, with an exposed off-white axis. Main stem about 9 mm long before first branch, and 5 mm in diameter at base. Branches up to 10 cm in length and 0.6–2.0 mm in diameter. Polyps 0.5–4.0 mm long and 0.5–2.5 mm wide.

Type locality: An unnamed seamount located on the Caroline Ridge, 814 m.

Etymology: The Latin adjective *elegans* (elegant) refers to the beautiful external appearance of this

species.

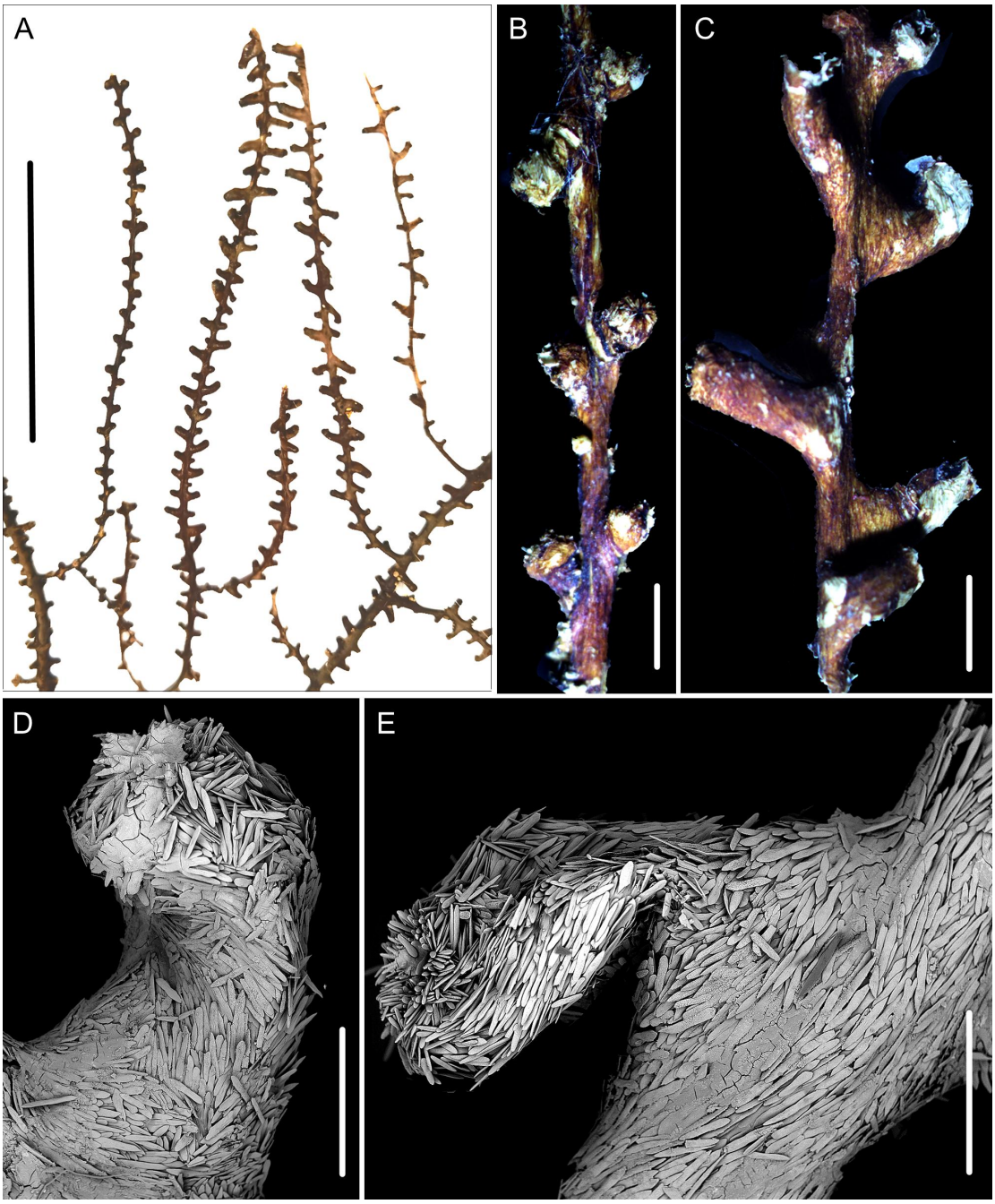

Figure 19 Branches and polyps of *Isidoides elegans* sp. nov. (A) branches of the paratype after fixation; (B, C) two parts of branches with wart-like and tubular polyps under a light microscope, respectively; (D, E) single tubular and wart-like polyp under SEM, respectively. Scale bars: 5 cm (A), 2 mm (B, C), 1 mm (D, E).

Distribution and habitat: Found on the seamounts located on the Caroline Ridge in the tropical Western Pacific with water depths of 814–962 m. The colony grows on a rocky substrate, but may still survive when detached from their holdfast (Fig. 18A, D). At the site of collection, the water temperature was 5.31–5.65°C and the salinity about 36.8 psu.

Remarks: *Isidoides elegans* sp. nov. is similar to *I. armata* Nutting, 1910 in having varied polyp sizes and some bud-like polyps with enlarged distal ends, but differs in having sclerites with a non-granulated appearance (vs. granulated), flattened rods in tentacles (vs. rods) and sclerites in the polyp body and coenenchyme that are slender and often spindle-like (vs. relatively broad and often with two rounded ends)

(Table 5). The new species is also similar to *Isidoides incrassata* sp. nov. in color, but differs by the size and shape of polyps (tubular and wart-like, up to 6 mm *vs.* conical and tubular, up to 3 mm), polyps being usually biserially arranged (*vs.* densely arranged on all sides of the branches), thin rods with a non-ridged surface in tentacles (*vs.* thick rods with ridged surface), and flat rods in the polyp body wall and coenenchyme with a non-granulated surface (*vs.* densely granulated).

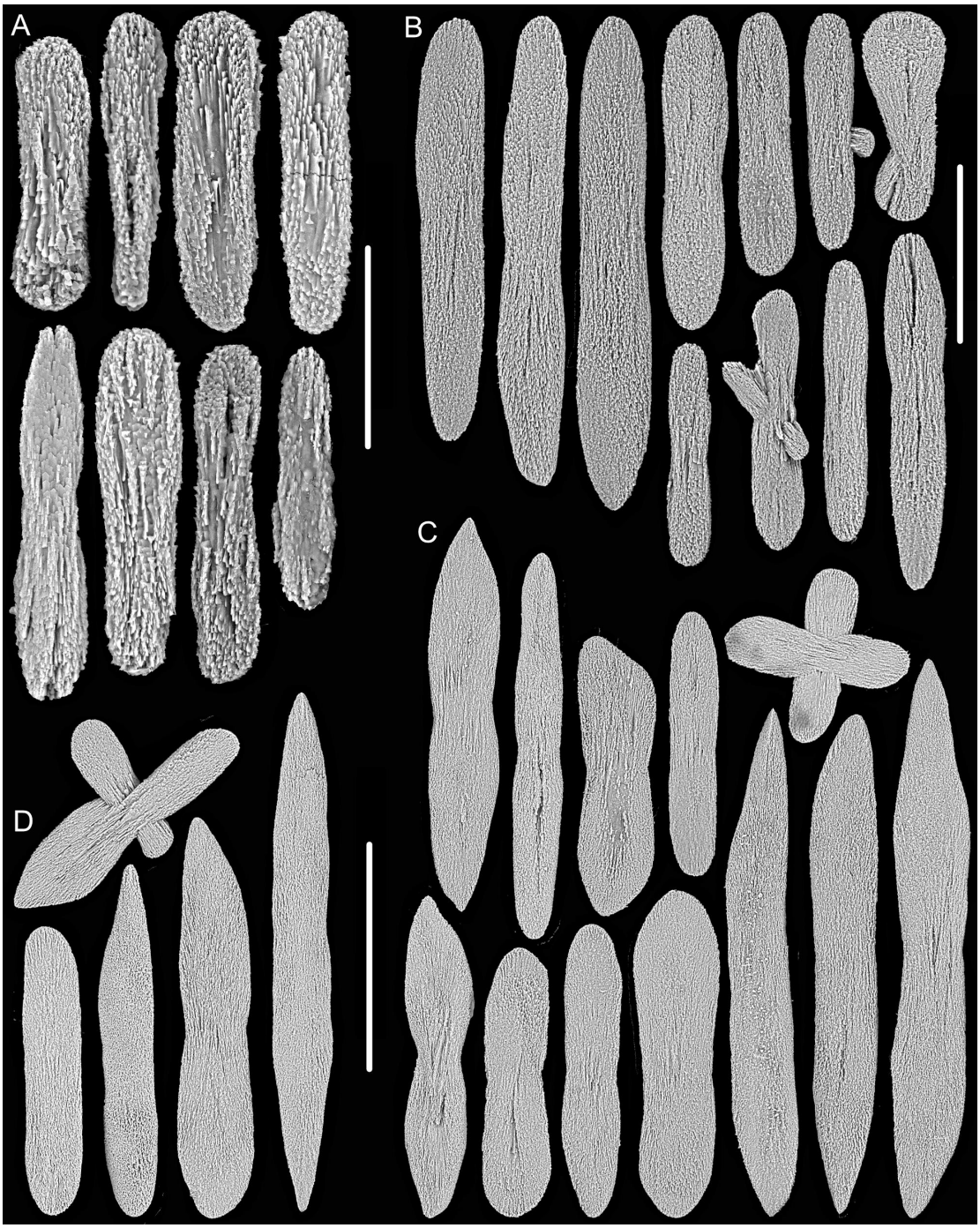

Figure 20 Sclerites of *Isidoides elegans* sp. nov. (A, B) small and large sclerites in tentacles; (C) sclerites in polyp body wall; (D) sclerites in coenenchyme. Scale bar: 200 µm (C, D in the same scale), 100 µm (B), 50 µm (A).

***Isidoides gracilis* Xu, Bilewitch & Pante sp. nov.**

Figs. 4B, C, P; 21–27

urn:lsid:zoobank.org:act:EC68E605-622F-4CB4-8FA9-13D8FCD00A6B

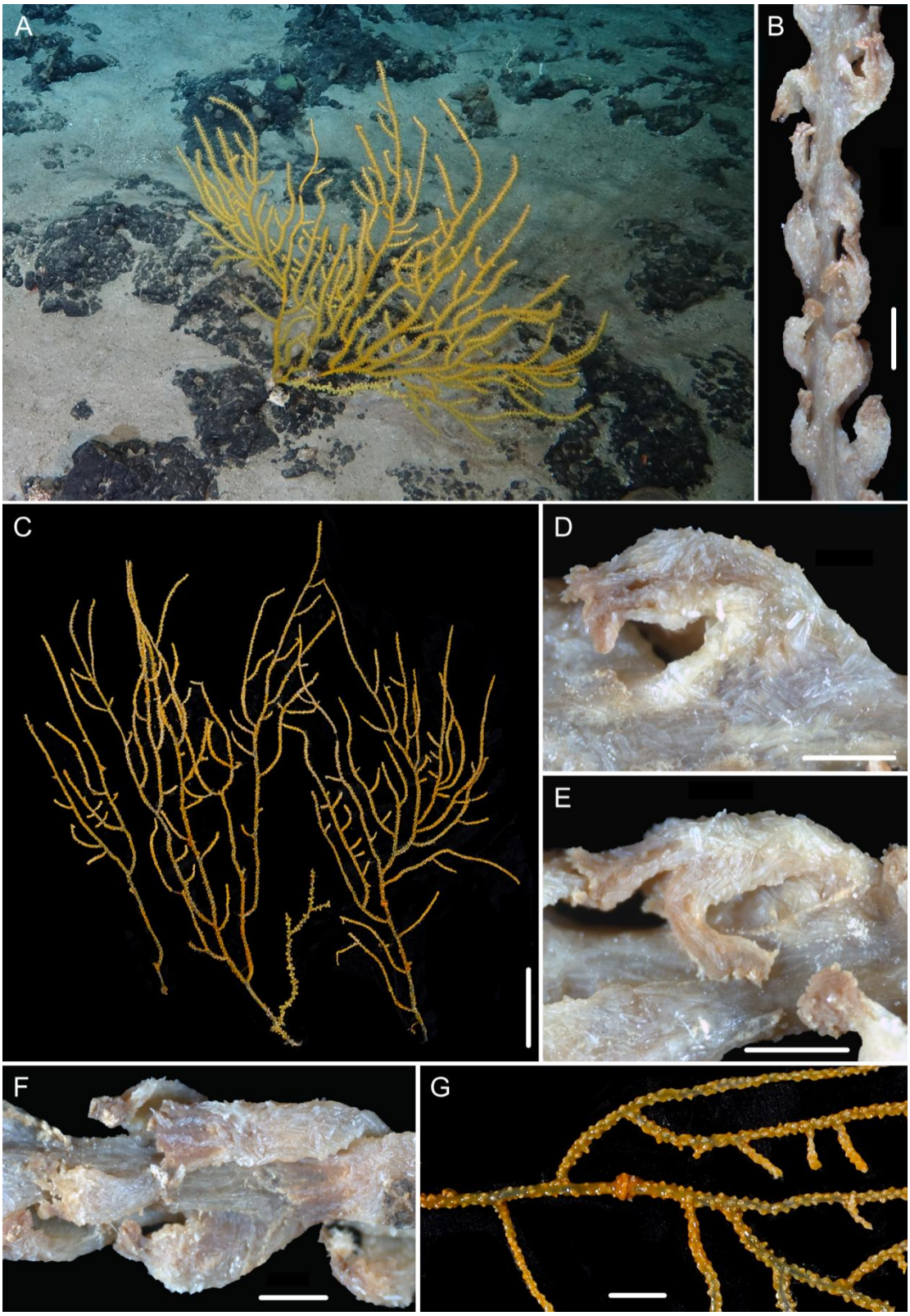

Figure 21 External morphology of the holotype of *Isidoides gracilis* sp. nov. form 1. (A, C) the specimen *in situ* and after collection, respectively; (B, F) part of terminal branchlet under a light microscope; (D, E) single polyps under under a light microscope; (G) part of branch with abundant wart-like polyps and a swollen protrusion. Scale bars: 10 cm (C), 2 cm (G), 2 mm (B), 1 mm (D, E, F).

Material examined: Holotype: MBM286877, station FX-Dive 308 (15°02′55″N, 116°33′29″E), Zhenbei Seamount in the central South China Sea, 797 m, 20 July 2022. **Paratypes**: MBM286878, the Ganquan Plateau in the northwest South China Sea, 586–910 m, 14 June 2018. MBM286879, 22°02′06N, 118°46′33E, close to a submarine hydrothermal solution in the northern South China Sea, 811 m, September 2016. MBM286880, the same location and date with MBM286879, depth unknown.

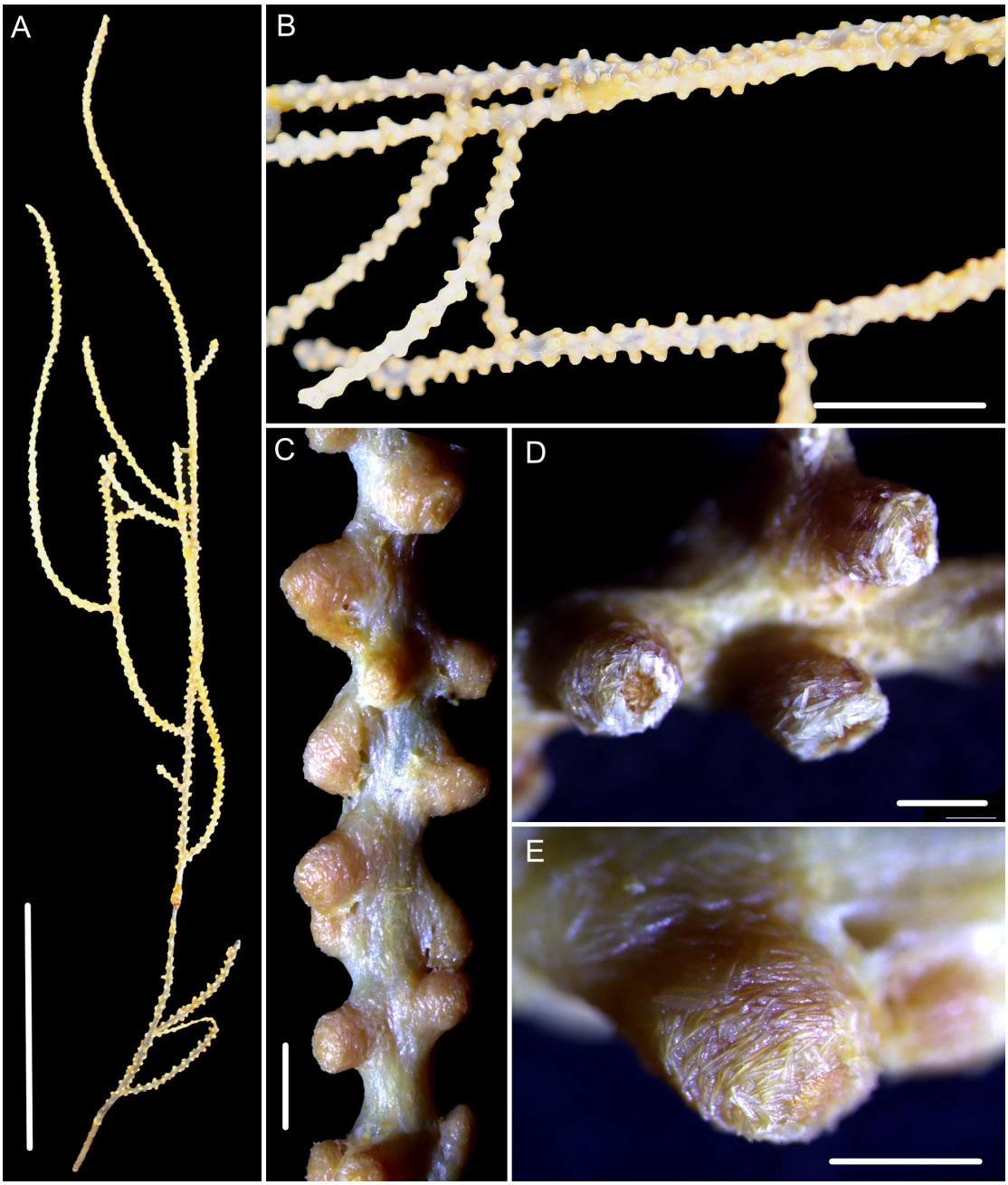

Figure 22 External morphology and polyps of the paratype MBM286878 of *Isidoides gracilis* sp. nov. form 1. (A) the specimen after collection; (B) close-up branches; (C, D) part of branches with polyps under a light microscope; (E) single polyp under a light microscope. Scale bars: 10 cm (A), 2 cm (B), 2 mm (C), 1 mm (D, E).

Diagnosis: Colony planar with a gray to dark brown axis, yellow when alive and gray to brown after fixation. In juvenile colony, polyps uniformly tubular and arranged biserially on each side of branches. In adults, polyps vary greatly in size and shape, including small and wart-like and densely arranged in an irregular series on main stem and large branches, and large and tubular and biserially arranged in

branchlets. Sclerites almost flattened rods, occasionally crossed-shaped, often with a slight medial constriction and a non-granulated surface.

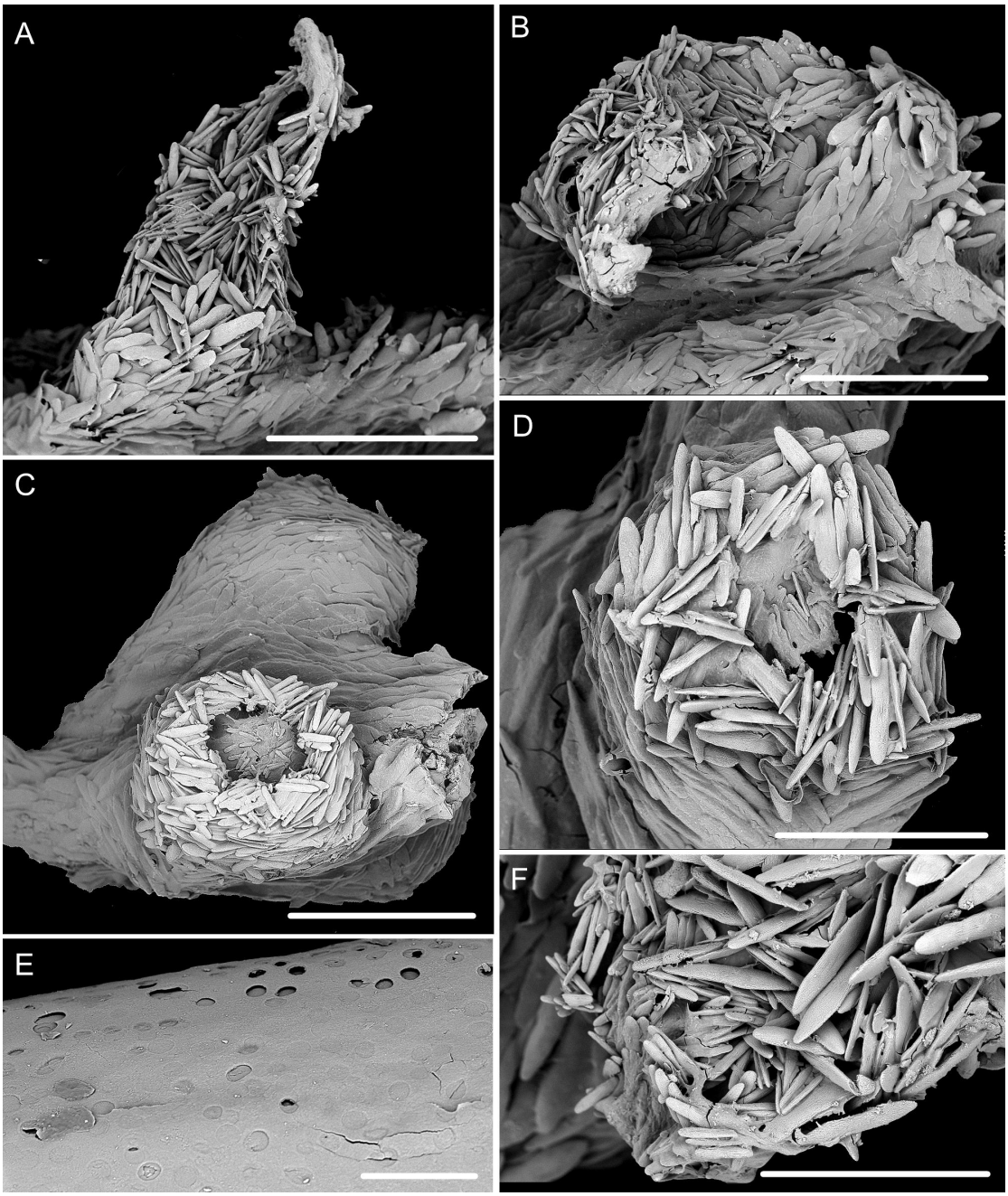

Figure 23 Polyps and axis of *Isidoides gracilis* sp. nov. form 1 under SEM. (A, B) single tubular polyps of holotype; (C) two wart-like polyps of MBM286878; (D) head of the wart-like polyp; (E) surface of branch axis in MBM286878; (F) tentacular part of a tubular polyp. Scale bars: 1 mm (A–C), 500 µm (D, F), 100 µm (E).

Morphology of *I. gracilis* sp. nov. form 1 (specimens MBM286877, MBM286878 and MBM286879): Holotype MBM286877 planar, yellow to light brown in life and light brown after fixation, about 65 cm in height (Fig. 21A). Holdfast large and white in situ but not collected. Stem about 4 mm at base, occasionally with a swollen protrusions (Fig. 22G). The central axis round and dark brown, lighter in colour in branches, sometimes became nearly black and a little flat, and abundant small and round pits can be seen on surface under SEM (Fig. 23E). Branches gracile and flexible, irregularly and pseudo-dichotomously branched in one plane and without anastomosis (Fig. 21A, C). Distance between the

adjacent branches 0.5–11.5 cm long, and the terminal branchlets up to 21 cm long.

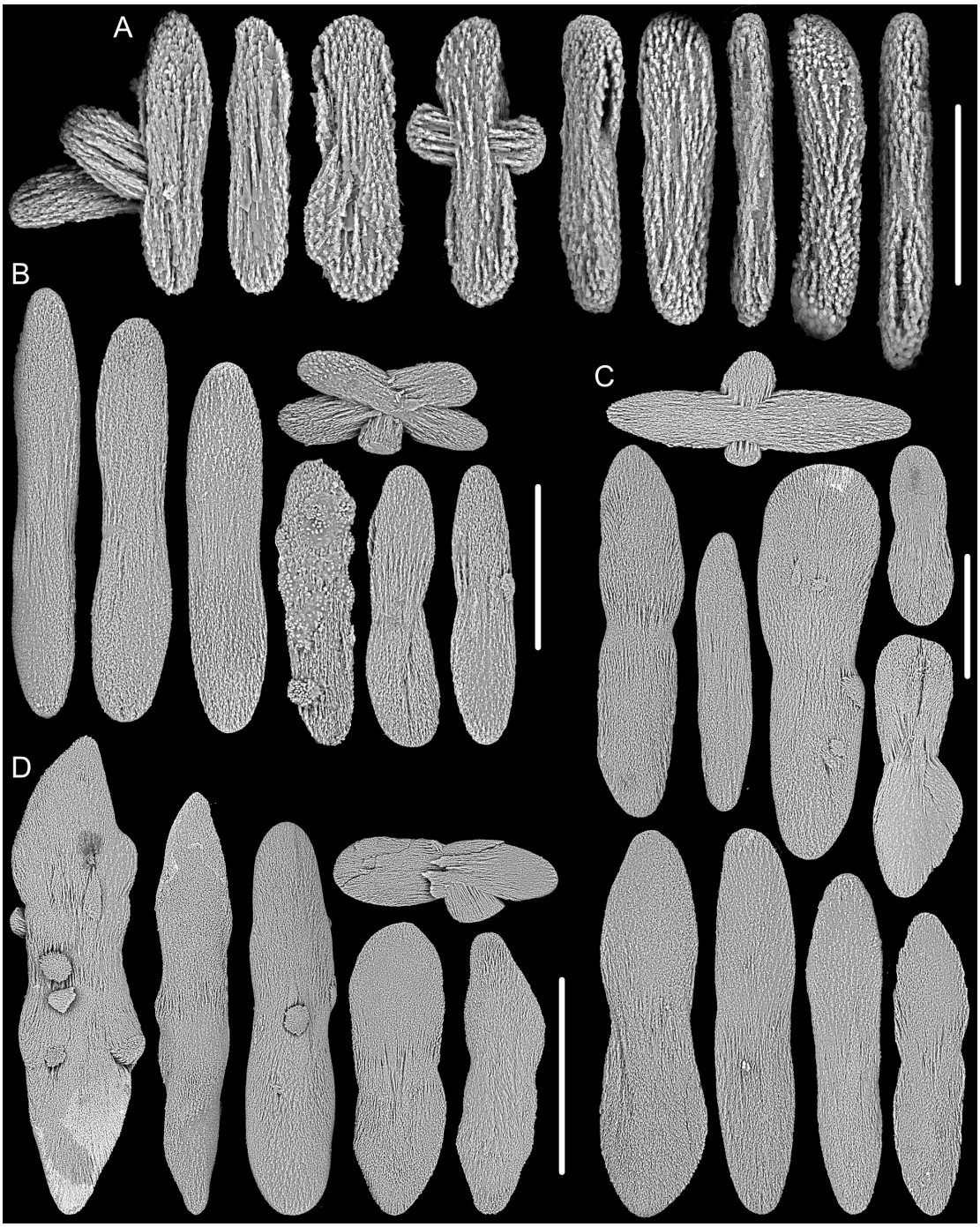

Figure 24 Sclerites of *Isidoides gracilis* sp. nov. form 1. (A, B) small and large sclerites in tentacles, respectively; (C) sclerites in polyp body wall; (D) sclerites in coenenchyme. Scale bar: 200 μm (D), 100 μm (B, C), 50 μm (A).

Polyps vary in size and shape, including large tubular (Fig. 21D, E) and small wart-like (Fig. 21G), 1.0–3.5 mm long, 1.0–1.5 mm wide. Among them, small wart-like polyps usually irregularly and densely arranged on all sides of the main stem and large branches (Fig. 21G), while large tubular polyps irregularly arranged in the terminal branches, sometimes biserially and alternately arranged (Figs. 21B, F). Polyps with an opaque body wall, firmly attached to the branch and did not easily detach off the colony after fixation. Tentacles usually extended in large tubular polyps (Fig. 21D–F) and tightly folded into the oral disc in small wart-like polyps (Fig. 21G).

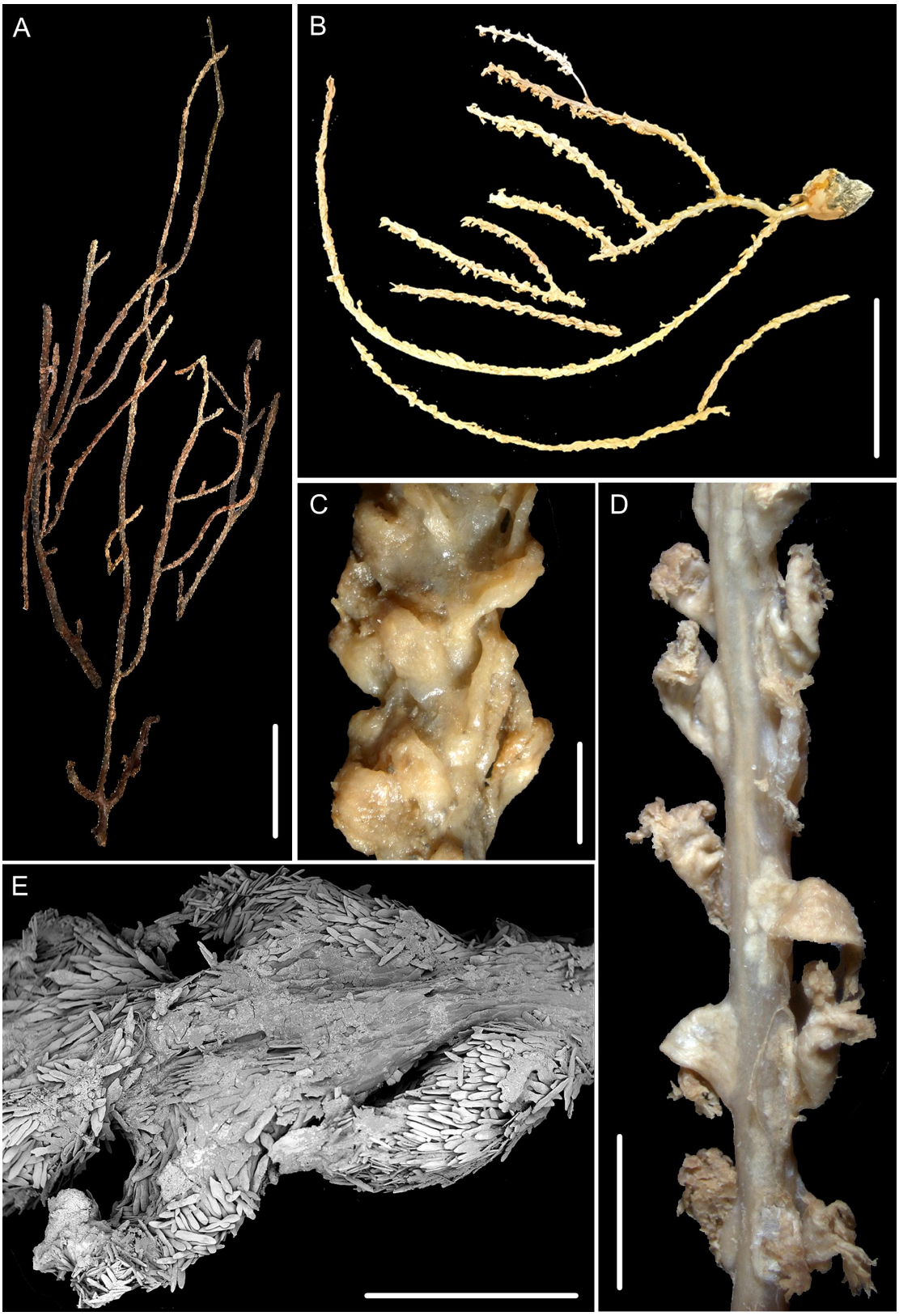

Figure 25 External morphology and polyps of *Isidoides gracilis* sp. nov. (A, B) MBM286879 (form 1) and MBM286880 (form 2) after fixation, respectively; (C, D) part of branch of MBM286879 and MBM286880 after fixation under a light microscope, respectively; (E) part of branch with polyps of MBM286880 under SEM. Scale bars: 10 cm (A), 5 cm (B), 2 mm (C–E).

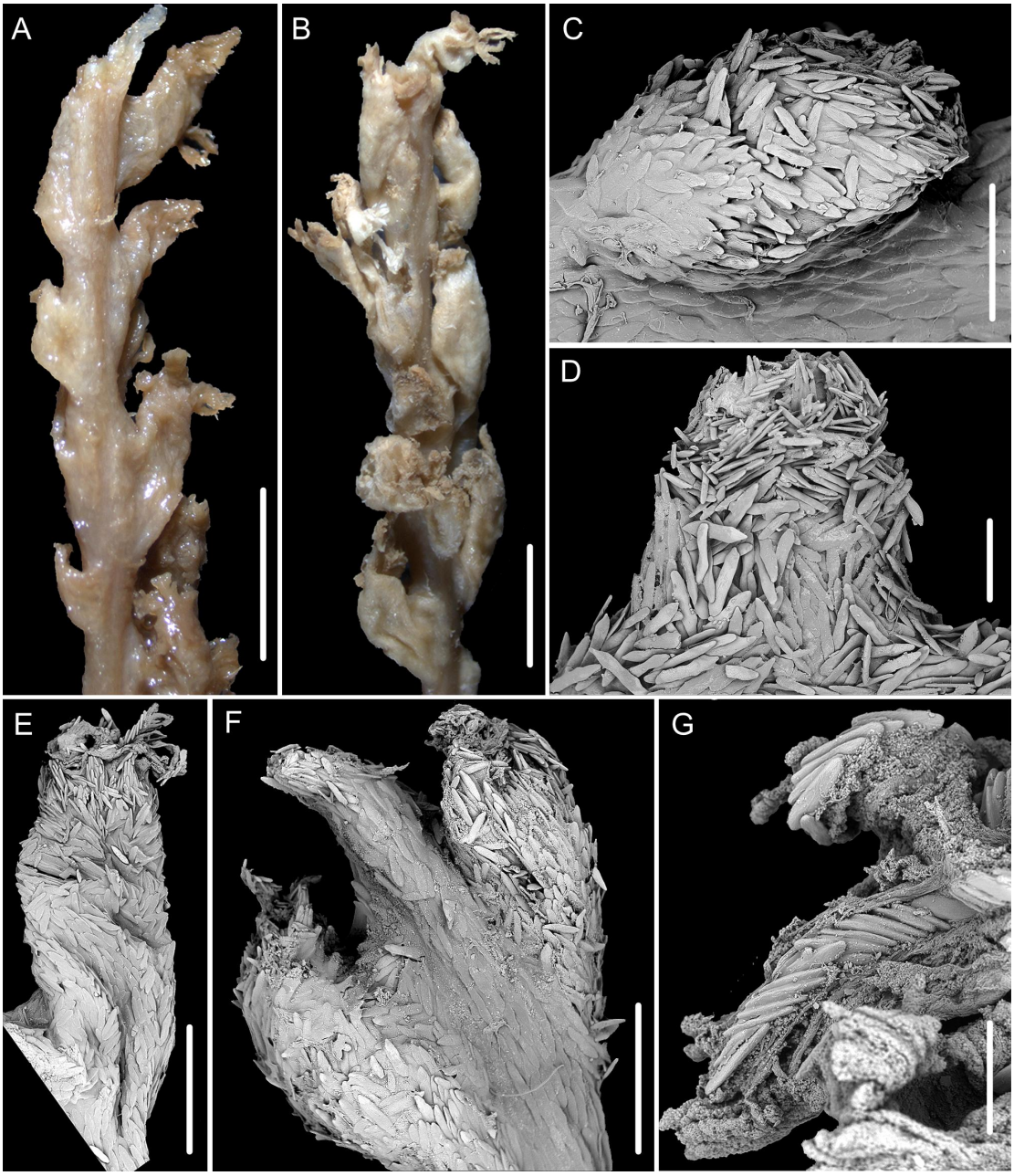

Figure 26 Branches and polyps of *Isidoides gracilis* sp. nov. (A, B) part of branch of MBM286880 (form 2) after fixation under a light microscope; (C, E, F) tubular polyps of MBM286880 under SEM; (D) small tubular polyp of MBM286879 (form 1) under SEM; (G) tentacular part covered with sclerites of MBM286880 under SEM. Scale bars: 2 mm (A, B), 1 mm (E, F), 500 μm (C, D), 200 μm (G).

Polyps and coenenchyme covered with dense sclerites (Fig. 23). Sclerites are almost flattened rods, often with a slightly medial constriction and two rounded ends, occasionally crossed-shaped or with large warts and grooves (Fig. 24). Their profiles mostly smooth, and surface usually non-granulated, striped, lamellar or of mixed shapes, rarely feather-shaped, occasionally sparsely granulated in small sclerites of tentacles (Figs. 4H–K, 24). Rods and flattened rods in the back of the tentacle rachis slender, longitudinally or irregularly arranged, some branched with irregular shapes, and measuring 71–262 × 8–52 μm (Figs. 23A, B, F; 24A, B). Flattened rods in the polyp body wall transversely or obliquely arranged, and measuring 143–419 × 22–130 μm (Fig. 24C). Sclerite forms in the coenenchyme same as the polyp body wall, but relatively thick and large, arranged along the branch, and measuring 113–488 × 34–204 μm (Fig. 24D).

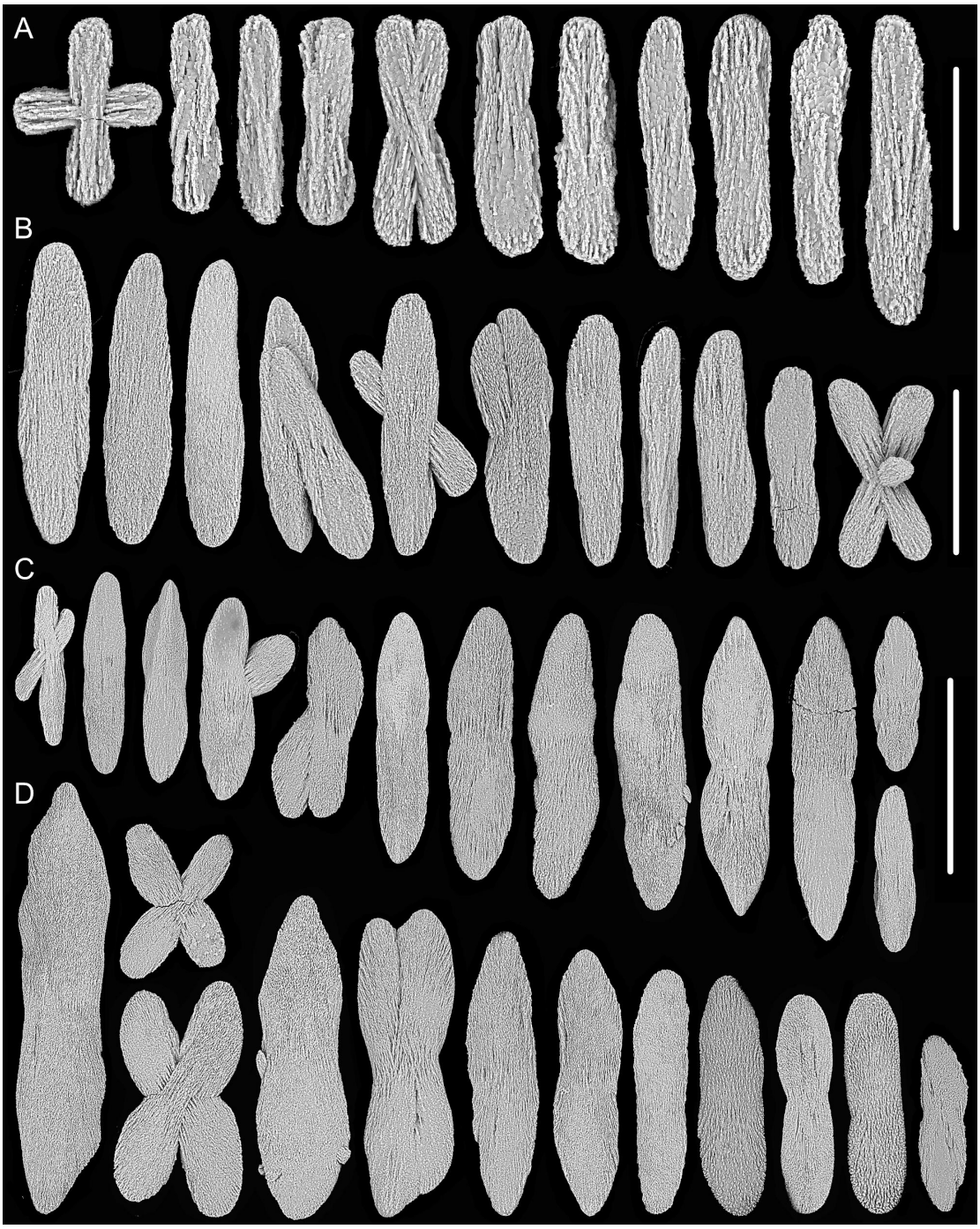

Figure 27 Sclerites of *Isidoides gracilis* sp. nov. form 2 (specimen MBM286880). (A) small sclerites in tentacles; (B) large sclerites in tentacles; (C) sclerites in the polyp body wall; (D) sclerites in coenenchyme. Scale bar: 200 µm (C, D in the same scale), 100 µm (B), 50 µm (A).

The paratype MBM286878 incomplete with only a small part of the specimen obtained. The original specimen yellow, about 48 cm in height with the holdfast not recovered as seen on the picture after collection (Fig. 22A). The polyps all small wart-like, irregularly and densely arranged on each side of the stem and branches, 0.5–1.0 mm long and up to 2 mm apart (Fig. 22A). Tentacles tightly folded into the oral disc, forming a dome shape (Fig. 22C, E), sometimes concave inward forming a central concavity (Figs. 22D; 23C, D).

The paratype MBM286879 incomplete with the holdfast not recovered, deep brown after fixation, and about 65 cm in height (Fig. 25A). Stem about 9 mm at the base. The central axis round and brown at the

stem and became flattened and dark gray in branches, occasionally nearly black and with swollen protrusions. The terminal branchlets up to 21 cm long. Polyps 1.0–4.0 mm long, 1.0–1.5 mm wide, usually tubular, soft and twisted, some of them wart-like in the main stem (Figs. 25A, C, 26D). Polyps densely arranged on each side of the main stem and branches, occasionally biserially and relatively sparse on branchlets, up to 1.0 mm apart and oriented toward the distal end (Fig. 25C, E). Tentacles contractile and almost extended, occasionally tightly folded forming a wart-like shape.

Morphology of *I. gracilis* sp. nov. form 2 (specimen MBM286880): This specimen small, about 10.5 cm in height and gray to brown in color after fixation (Fig. 25B). Holdfast oval-shaped, about 1.8 cm in diameter. Stem about 3 mm in diameter at base with a round gray central axis, and about 6 mm before branched. Branches sparsely branched with inter-distance 1.6–4.7 cm. Polyps soft and uniformly tubular with extended tentacles, 1.0–6.0 mm long, 1.0–1.5 mm wide, arranged biserially on each side of branches (Figs. 25D, 26A, B).

Sclerites are flattened rods, often with a slightly medial constriction, occasionally crossed-shaped and with large warts (Fig. 27). Their profiles relatively irregular, and surface usually non-granulated (e.g., Fig. 4H–K), occasionally with sparse granulated appearance. Sclerites in the back of the tentacle rachis arranged longitudinally, small and sometimes branched with irregular shape, and measuring 46–186× 11–83 μm (Figs. 26G; 27A, B). Sclerites in the polyp body wall longitudinally or arranged crosswise, and measuring 111–370 × 26–94 μm (Figs. 26C–F, 27C). Sclerites in coenenchyme similar to body wall but relatively large, and measuring 156–442× 38–131 μm (Fig. 27D).

Type locality: Zhenbei Seamount in the South China Sea, 797 m.

Etymology: The Latin adjective *gracilis* (gracile) refers to the gracile stem and branches of this species.

Distribution and habitat: Found from the South China Sea at water depths of 586–910 m. Colony was attached to a rocky substrate (Fig. 23A). The water temperature was 5.85°C and the salinity about 36.3 psu.

Remarks: The four specimens of *I. gracilis* sp. nov. can be classified into two forms and all have the same sclerite forms, characterized by a non-granulated appearance and frequently having a slightly medial constriction. Moreover, the phylogenetic analysis of Sanger and UCE sequences indicates they fall within the range of intraspecific differences (see the genetic analysis above). Thus, we identified the four specimens as the same species.

Minor differences between the two forms include (1) the form 2 (specimen MBM286880) has a small colony with a gray and round axis, while the specimens of form 1 all have a relatively large colony with a round and brown axis, sometimes become flattened and nearly black; (2) polyps of the form 2 are uniformly tubular and biserially arranged (Figs. 25D, 26A, B), while the form 1 are small wart-like or large tubular, and densely arranged on each side of main stem and branches, occasionally biserially on branchlets (Figs. 21, 22, 25A, C, E). These differences are not constant and possibly caused by different growth stages (form 2 is a juvenile and form 1 is likely an adult) or environmental conditions, and we thus treated them as conspecific variation.

Isidoides gracilis sp. nov. is similar to *I. pseudarmata* sp. nov. in being yellow when alive, but differs by its sclerites with an almost non-granulated surface (*vs.* granulated surface) in the polyp body wall and coenenchyme, flattened rods in tentacles (vs. rods), and tubular polyps always displaying extended tentacles in the preserved state (vs. tentacles tightly folded, forming a pseudo-operculum) (Table 5).

Discussion

High diversity of *Isidoides* Nutting, 1910

The morphological and phylogenetic analyses support the erection of four new species of *Isidoides*. The *mtMutS-cox1*, *28S rDNA* and UCE trees all support the establishment of *Isidoides elegans* sp. nov. (Figs. 1–3). *Isidoides gracilis* sp. nov. has two morphological forms and its specimens formed a single clade in *28S rDNA* and UCE trees with full support. Four forms of *I. armata* Nutting, 1910 were recognized with morphological variations in colony color and polyp shape, thickness and arrangement but all shared the same sclerite forms (Table 5) and are therefore treated as the same species. Unfortunately, the type specimen (lectotype) of *I. armata* Nutting, 1910 has been lost, and we failed to obtain sequence

data from the paralectotype. The remaining two forms clustered with *I. incrassata* sp. nov. with low support in both *mtMutS-cox1* and *28S* trees, which failed to resolve their phylogenetic affinities. However, *I. incrassata* sp. nov. formed a clade sister to all *I. armata* specimens with full branch support in UCE trees, supporting their separation although only a single specimen was sequenced. *Isidoides pseudarmata* sp. nov. is a new species separated from *I. armata,* and its five specimens formed a single clade with full support in *28S rDNA* and UCE trees.

Based on available evidence, we propose five valid species of *Isidoides*, including *I. armata* Nutting, 1910, *I. elegans* sp. nov., *I. gracilis* sp. nov., *I. incrassata* sp. nov. and *I. pseudarmata* sp. nov. Considering the external morphological variations, other specimens such as C014597 (*Isidoides* sp. 1 in Table 3, collected and identified as "*I. armata*" by Phil Alderslade), NIWA16239 and NIWA41714 (*Isidoides* sp. 2 in Table 3, stored in NIWA Invertebrate Collection) need further examination of sclerite morphology and phylogenetic position. All of the known *Isidoides* specimens have been found and distributed in the Indo-West Pacific and southwest Pacific at water depths of 424–1065 m, showing an unexpected high diversity (Table 3; Nutting, 1910; Pante et al., 2013; present study).

The distributional patterns of *Isidoides* species suggest that latitude plays a greater role than depth in structuring species ranges (Fig. 28). Four species—*I. elegans* sp. nov., *I. gracilis* sp. nov., *I. pseudarmata* sp. nov. and *I. incrassata* sp. nov.—are largely separated by latitude, whereas *I. armata*, the best-sampled species, exhibits the broadest latitudinal distribution. Its range overlaps with that of *I. pseudarmata* sp. nov. in New Caledonia and with *I. incrassata* sp. nov., underscoring its comparatively wide ecological amplitude. In contrast, depth appears to be of secondary importance, as the bathymetric ranges of most species overlap substantially. Notably, *I. armata* stands out for its extensive distribution, both latitudinally and bathymetrically. However, these patterns must be interpreted with caution, since sample sizes remain low across species, including for *I. armata*, the species represented by the largest number of records.

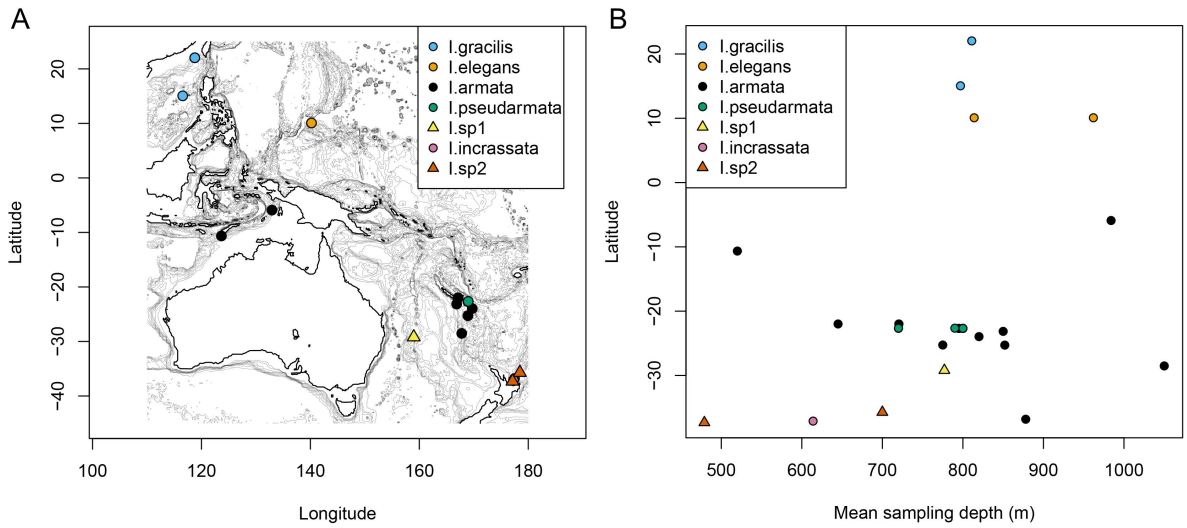

Figure 28 Geographic and bathymetric distribution of *Isidoides* species. (A) map showing the collection localities of all examined *Isidoides* specimens across the Indo-West Pacific and southwest Pacific; (B) mean sampling depth versus latitude for each species, illustrating latitudinal separation among most taxa and overlapping bathymetric ranges.

Comparison of the phylogenetic resolution of mitochondrial genes (*mtMutS-cox1*), nuclear genes (*28S*) and ultraconserved elements (UCEs)

Recent studies have shown that mitochondrial genes (e.g., *mtMutS*, *cox1*) exhibit low efficiency in distinguishing octocoral species, whereas the nuclear gene *28S rDNA* performs well (e.g., Xu et al., 2021a, b; Baena et al., 2024). Consistent with these findings, our study reveals that the concatenated *mtMutS-cox1* dataset only distinguishes *I. elegans* sp. nov. and fails to resolve phylogenetic relationships among most *Isidoides* species (Fig. 1). In contrast, *28S rDNA* distinguishes four species but cannot clarify the relationship between *I. armata* and *I. incrassata* sp. nov. (Fig. 2).

UCE sequences obtained through target-capture enrichment and genome skimming are emerging molecular markers capable of resolving higher-level taxonomic relationships, however, examples of their application at the species level remain limited (Erickson et al., 2020; Untiedt et al., 2021; McFadden et al., 2022). In this study, UCEs successfully distinguished all *Isidoides* species with high support (Fig. 3), including *I. armata* and *I. incrassata* sp. nov., which exhibit clear morphological differences but were indistinguishable by *28S rDNA*. UCEs thus outperform both nuclear gene (*28S rDNA)* and mitochondrial genes (*mtMutS-cox1*) in resolving the phylogeny of *Isidoides* species. For species delimitation, UCEs are highly effective at detecting similar species exhibiting some limited morphological divergence but their use without such complementary evidence may lead to inflated species diversity estimates where intra-specific variation may be mistaken for species-level differences (e.g., Erickson et al., 2020).

Important features for species delimitation of *Isidoides*

Some commonly used taxonomic characters, such as color, polyp shape, size and arrangement, etc., are less useful for the species identification of *Isidoides*, due to intraspecific morphological variations (phenotypic plasticity). In the specimens of *I. armata*, four morphological forms can be separated based on colony color (white, very light brown, brown); polyp shape (tubular, club-shaped, wart-like), thickness (opaque and thick or translucent and thin) and arrangement (biserial, or irregular); tentacular expansion (or not); and ultrastructure of the sclerites on the surface of the polyp body and coenenchyme (non-granulated, slightly granulated or densely granulated) (Table 5).

Variation in sclerite morphology is usually regarded as an important feature for octocoral species identification (e.g., Versluys, 1902; Xu et al., 2021a). In the genus *Isidoides*, all species have rod-like sclerites with relatively uniform size. Only a few microstructural differences of the sclerite surface (granulated and ridged or not), the tentacle sclerites (rods or flattened rods), and the shape of polyp body and coenenchymal sclerites (often slender and spindle-like or relatively broad with two rounded ends and a slightly medial constriction) can be recognized. Based on the morphological and phylogenetic analysis of *Isidoides*, axis color, sclerites in the tentacles and surface sculpturing of sclerites (see Fig. 4) all show differences and are important features for *Isidoides* species identification. However, with the exception of *I. armata*, few representative specimens of each new species were available for examination. Further sampling is required to determine how much phenotypic variation exists in these diagnostic characters, which may occur over environmental clines such as depth or latitude or in response to preservation conditions.

Based on the morphological features as mentioned above, a key is given to distinguish the *Isidoides* species:

1. Thin and flattened rods in tentacles; surface of the sclerites in polyp body and coenenchyme almost non-granulated.....2
- Thick and stout rods in tentacles; surface of the sclerites in polyp body and coenenchyme more or less granulated.....3
2. Sclerites in polyp body wall and coenenchyme slender and often with two acute ends; polyps usually loosely and biserially arranged; colony deep brown to ochre when alive.....*I. elegans* sp. nov.
- Sclerites in polyp body wall and coenenchyme relatively stout and often with two rounded ends; polyps usually densely arranged on all sides; colony yellow when alive.....*I. gracilis* sp. nov.
3. Surface of tentacles sclerites ridged and/or granulated; axis white, cream-coloured to light brown.....4
- Surface of tentacles sclerites non-ridged and non-granulated; axis dark golden-brown to black.....*I. pseudarmata* sp. nov.
4. Sclerites in polyp body wall and coenenchyme slender bar-like; polyps usually small conical, irregularly and densely arranged on all sides; colony deep ochre after fixation.....*I. incrassata* sp. nov.
- Sclerites in polyp body wall and coenenchyme relatively stout often with a slightly medial constriction; polyps usually large tubular and biserially arranged, occasionally irregularly on all sides; colony cream-coloured to light brown after fixation..... *I. armata* Nutting, 1910

Summary

This study described four new species and redescribed one known species of *Isidoides* Nutting, 1910, including *I. elegans* sp. nov., *I. gracilis* sp. nov., *I. incrassata* sp. nov., *I. pseudarmata* sp. nov. and *I. armata*. The morphological analysis showed *Isidoides* species have high intraspecific morphological variation in colony color and polyps, and the sclerite forms with their surface sculpture are important features for species identification. The phylogenetic analysis indicated that UCE phylogenomics has higher resolution than the *28S rDNA* and the mitochondrial *mtMutS* and *cox1* for species delimitation.

Conclusion

Phylogenomic approaches represent a powerful means to distinguish closely related and morphologically similar species. The discovery of four new species hidden within a previously monospecific family, combined with the observed inability of single-locus barcodes to adequately distinguish these similar species indicates that, despite past molecular systematic efforts many new octocoral species await discovery in the deep-sea.

Funding

This work was supported by the National Natural Science Foundation of China (No. 41930533, 42306102, 42176128), the National Key Research and Development Program of China (2021YFE0193700), Shandong Provincial Natural Science Foundation (ZR2024QD241), the Postdoctoral Innovation Talents Support Program of Shandong (SDBX2022027). NIWA registered specimens were provided from the NIWA Invertebrate Collection and were collected by scientific observers on commercial fishing vessels funded by Fisheries New Zealand, and on research survey TAN1206 as part of the "Impact of resource use on vulnerable deep-sea communities" project funded by the former New Zealand Foundation for Research, Science and Technology.

Acknowledgements

We are grateful to the crew and technicians of RV KEXUE (https://cstr.cn/31114.02.MORV) for providing support and assistance in data and sample collection. We thank Dr. Jiehong Wei for his guidance on phylogenetic analysis. We also appreciate the editor for his editorial work and reviewers for their constructive comments on an early version of the manuscript.

New Zealand specimens collected by NIWA during voyages KAH0011 and TAN0413 "Seamounts: their importance to fisheries and marine ecosystems" and TAN1206 "Impact of resource use on vulnerable deep-sea communities" were funded by the former New Zealand Foundation for Research, Science and Technology (CO1X0028/0224 (SFAS013/033) and CO1X0906) with additional funding from the Ministry of Fisheries (ZBD2004-01) and NOAA Satellite Operations Facility (NRAM053). An additional New Zealand specimen from station Z9224 was collected under the Scientific Observer Program funded by the New Zealand Ministry for Primary Industries (Fisheries).

The specimens hosted at the MNHN were sampled within the framework of the 'Tropical Deep-Sea Benthos' research program (formerly MUSORTSOM), spearheaded by the MNHN and the IRD (Bouchet et al., 2008). We are grateful to the scientists and crews of the following cruises for their sampling efforts and at-sea support: TERRASSE (R/V Alis; chief scientist Sarah Samadi; 16 Oct–31 Oct 2008; DOI: 10.17600/8100100), EXBODI (R/V Alis; chief scientists Sarah Samadi and Laure Corbari; 28 Aug–29 Sep 2011; DOI:10.17600/11100080), NORFOLK2 (R/V Alis; chief scientist Bertrand Richer de Forges; 20 Oct–06 Nov 2003; DOI: 10.17600/3100030), and BIOCAL (R/V Jean Charcot; chief scientist Claude Lévi; 08 Aug–10 Sep 1985; DOI: 10.17600/85002911). We also thank Magalie Castelin for assistance with the MNHN collections. Financial support for collection in New Caledonia during TERRASSE was provided by Sigma Xi (GIARG20061021830514629), the American Museum of Natural History (Lerner Gray Fund) and NSF (EF-0531570; EF-0531779), and the French Société Francaise d'Écologie. All material has been collected under appropriate collection permits and approved ethics guidelines (detailed in Pante et al.,

2012).

Conflict of interest disclosure

The authors declare that they comply with the PCI rule of having no financial conflicts of interest in relation to the content of the article.

References

Aberer, A.J., Kobert, K., Stamatakis, A. (2014) ExaBayes: massively parallel Bayesian tree inference for the Whole-Genome Era. *Molecular Biology and Evolution*, 31, 2553–2556. https://doi.org/10.1038/s42003-021-02348-y.

Alfaro, M.E., Zoller, S., Lutzoni, F. (2003) Bayes or Bootstrap? A simulation study comparing the performance of Bayesian Markov chain Monte Carlo sampling and bootstrapping in assessing phylogenetic confidence. *Molecular Biology and Evolution*, 20 (2), 255–266. https://doi.org/10.1093/molbev/msg028

Baena, P., Martell, L., Soto-Angel, J.J., Ambroso, S., López-González P.J. (2024) A new deep-sea species of golden gorgonian (Octocorallia: Scleralcyonacea: Chrysogorgiidae) from Antarctic waters. *Deep-sea Research Part I*, 204, 104234. https://doi.org/10.1016/j.dsr.2024.104234

Bankevich, A., Nurk, S., Antipov, D., Gurevich, A.A., Dvorkin, M., Kulikov, A.S., Lesin, V.M., Nikolenko, S.I., Pham, S., Prjibelski, A.D., Pyshkin, A.V., Sirotkin, A.V., Vyahhi, N., Tesler, G., Alekseyev, M.A., Pevzner, P.A. (2012) SPAdes: a new genome assembly algorithm and its applications to single-cell sequencing. *Journal of Computational Biology*, 19, 455–477. https://doi:10.1089/cmb.2012.0021

Bayer, F.M., Grasshoff, M., Verseveldt, J. (1983) Illustrated Trilingual Glossary of Morphological and Anatomical Terms Applied to Octocorallia. E. J. Brill/Dr. W. Backhuys, Leiden, 75 pp.

Bayer, F. (1979) *Distichogorgia sconsa*, a new genus and species of chrysogorgiid octocoral (Coelenterata: Anthozoa) from the Blake Plateau off Northern Florida. *Proceedings of the Biological Society of Washington*, 92, 876–882.

Bayer, F.M. (1981) Key to the genera of Octocorallia exclusive of Pennatulacea (Coelenterata: Anthozoa), with diagnoses of new taxa. *Proceedings of the Biological Scoiety of Washington*, 94 (3), 902–947.

Bayer, F., Grasshoff, M. (1994) The genus group taxa of the family Ellisellidae, with clarification of the genera established by J. E. Gray (Cnidaria: Octocorallia). *Senkenbergiana biologica*, 74, 21–45.

Bayer, F., Stefani, J. (1988) A new species of *Chrysogorgia* (Octocorallia: Gorgonacea) from New Caledonia, with descriptions of some other species from the Western Pacific. *Proceedings of the Biological Society of Washington*, 101, 257–279.

Bouchet, P., Héros, V., Lozouet, P. & Maestrati, P. (2008) A quarter-century of deep-sea malacological exploration in the South and West Pacific: where do we stand? How far to go? In: Héros, V., Cowie, R.H. & Bouchet, P. (eds) Tropical Deep-Sea Benthos 25, Mémoires du Muséum national d'Histoire naturelle, 196, 9–40. Paris ISBN: 978-2-85653-614-8.

Buhl-Mortensen, L., Mortensen, P.B. (2005) Distribution and diversity of species associated with deep-sea gorgonian corals off Atlantic Canada. In: Freiwald, A., Roberts, J.M. (eds) Cold-Water Corals and Ecosystems. Erlangen Earth Conference Series. Springer, Berlin, Heidelberg. https://doi.org/10.1007/3-540-27673-4_44

Dautova T.N. (2019) Octocorallia as a key taxon in the vulnerable marine ecosystems of the Emperor Chain (Northwest Pacific): diversity, distribution and biogeographical boundary. In: K.A. Lutaenko (ed.). Marine Biodiversity for a Healthy Ocean – Biodiversity, Functional Groups and Ocean Health.

Proceedings of the Russia-China Bilateral Workshop, October 10–11, 2019, Vladivostok, Russia. Vladivostok: Publishing House of the Far Eastern Federal University. P.68–80.

Ehrenberg, C.G. (1834) Beiträge zur physiologischen Kenntniss der Corallenthiere im allgemeinen, und besonders des rothen Meeres, nebst einem Versuche zur physiologischen Systematik derselben. *Abhandlungen der Königlichen Akademie der Wissenschaften, Berlin*, 1, 225–380.

Erickson, K., Pentico, K., Quattrini, A.M. & McFadden, C.S. (2020) New approaches to species delimitation and population structure of anthozoans: two case studies of octocorals using ultraconserved elements and exons. *Molecular Ecology Resources*, 21, 78–92. https://doi: 10.1101/2020.04.01.021071

Faircloth, B.C. (2015) PHYLUCE is a software package for the analysis of conserved genomic loci. *Bioinformatics*, 32, 786–788. https://doi:10.1093/bioinformatics/btv646

Folmer, O., Black, M., Hoeh, W., Lutz, R., Vrijenhoek, R. (1994) DNA primers for amplification of mitochondrial cytochrome coxidase subunit I from diverse metazoan invertebrates. *Molecular Marine Biology and Biotechnology*, 3, 294–299.

Haeckel, E. (1866) Generelle morphologie der Organismen, vol. 2. Verlag von Georg Reimer, Berlin.

Hall, T.A. (1999) BioEdit: a user-friendly biological sequence alignment editor and analysis program for Windows 95/98/NT. *Nucleic Acids Symposium Series*, 41, 95–98.

Heestand Saucier, E., France, S.C., Watling, L. (2021) Toward a revision of the bamboo corals: Part 3, deconstructing the Family Isididae. *Zootaxa*, 5047 (3), 247–272. https://doi.org/10.11646/zootaxa.5047.3.2

Herrera, S., Baco, A., Sánchez, J.A. (2010) Molecular systematics of the bubblegum coral genera (Paragorgiidae, Octocorallia) and description of a new deep-sea species. *Molecular Phylogenetics and Evolution*, 55, 123–135. https://doi.org/10.1016/j.ympev.2009.12.007

Hillis, D.M., Bull, J.J. (1993) An empirical test of bootstrapping as a method for assessing confidence in phylogenetic analysis. *Systematic Biology*, 42 (2), 182–192. https://doi.org/10.1093/sysbio/42.2.182

Kalyaanamoorthy, S., Minh, B.Q., Wong, T.K.F., von Haeseler, A., Jermiin, L.S. (2017) ModelFinder: fast model selection for accurate phylogenetic estimates. *Nature Methods*, 14, 587–589.

Katoh, K., Standley, D.M. (2013) MAFFT multiple sequence alignment software version 7: improvements in performance and usability. *Molecular Biology and Evolution*, 30, 772–780.

Kessel, G.M., Alderslade, P., Bilewitch, J.P., Schnabel, K.E., Gardner J.P.A. (2022) The use of integrative taxonomy in Octocorallia (Cnidaria: Anthozoa): a literature survey. *Zoological Journal of the Linnean Society*, 2022, 198 (2), 677–690. https://doi.org/10.1093/zoolinnean/zlac099

Kimura, M. (1980) A simple method for estimating evolutionary rates of base substitutions through comparative studies of nucleotide sequences. *Journal of Molecular Evolution*, 16, 111–120.

Krieger, K.J., Wing, B.L. (2002) Megafauna associations with deepwater corals (*Primnoa* spp.) in the Gulf of Alaska. *Hydrobiologia*, 471, 83–90. https://doi.org/10.1023/A:1016597119297

Kumar, S., Stecher, G., Li, M., Knyaz, C., Tamura K. (2018) MEGA X: Molecular Evolutionary Genetics Analysis across computing platforms. *Molecular Biology and Evolution*, 35, 1547–1549.

Lanfear, R., Frandsen, P. B., Wright, A. M., Senfeld, T., Calcott, B. (2017) Partitionfinder 2: new methods for selecting partitioned models of evolution for molecular and morphological phylogenetic analyses. *Molecular Biology & Evolution*, 34 (3), 772–773.

McFadden, C.S., Benayahu, Y, Pante, E, Thoma, J.N., Nevarez, P.A., France, S.C. (2010) Limitations of mitochondrial gene barcoding in Octocorallia. *Molecular Ecology Resources*, 11, 19–31. https://doi.org/10.1111/j.1755-0998.2010.02875.x

McFadden, C.S., van Ofwegen, L.P. (2013) A second, cryptic species of the soft coral genus *Incrustatus* (Anthozoa: Octocorallia:Clavulariidae) from Tierra del Fuego, Argentina revealed by DNA barcoding. *Helgoland Marine Research*, 67, 137–147. https://doi.org/10.1007/s10152-012-0310-7

McFadden, C.S., Benayahu, Y., Pante, E., Thoma, J.N., Nevarez, P.A., France, S.C. (2011) Limitations of mitochondrial gene barcoding in Octocorallia. *Molecular Ecology Resources*, 11 (1), 19–31. https://doi: 10.1111/j.1755-0998.2010.02875.x

McFadden, C.S., Quattrini, A.M., Brugler, M.R., Cowman, P.F., Dueñas, L.F., Kitahara, M.V., Paz-García, D.A., Reimer, J.D., Rodríguez, E. (2021) Phylogenomics, Origin, and Diversification of Anthozoans (Phylum Cnidaria). *Systematic Biology*, 70 (4), 635–647. https://doi.org/10.1093/sysbio/syaa103

McFadden, C.S., van Ofwegen, L.P., Quattrini, A.M. (2022) Revisionary systematics of Octocorallia (Cnidaria: Anthozoa) guided by phylogenomics. *Bulletin of the Society of Systematic Biologists*, 1 (3), 8735. https://doi.org/10.18061/bssb.v1i3.8735

Morrissey, D., Lim, A., Howell, K.L., White, M., Wheeler, A.J., Allcock, A.L. (2023) The north-east Atlantic margin: A review of the geology, geography, oceanography, and vulnerable megabenthic ecosystems of the continental slope of Ireland and the United Kingdom. *Oceanography and Marine Biology: An Annual Review*, 61, 219–292. https://doi:10.1201/9781003363873-6

Nguyen, L.T., Schmidt, H.A., Von Haeseler, A., Minh, B.Q. (2015) IQ-TREE: a fast and effective stochastic algorithm for estimating maximum-likelihood phylogenies. *Molecular Biology and Evolution*, 32 (1), 268–274.

Nutting, C. (1910) The Gorgonacea of the Siboga Expedition VI. The Gorgonellidae. Siboga-Expeditie. Monograph XIIIb3.

Pante, E., France, S. C., Couloux, A., Cruaud, C., McFadden, C. S., Samadi, S., Watling, L. (2012) Deep-sea origin and in-situ diversi cation of chrysogorgiid octocorals. *PLoS ONE*, 7, e38357. https://doi:10.1371/journal.pone.0038357

Pante, E., Saucier, E.H., France, S.C. (2013) Molecular and morphological data support reclassification of the octocoral genus *Isidoides*. *Invertebrate Systematics*, 27, 365–378. http://dx.doi.org/10.1071/IS12053

Pante, E., Abdelkrim, J., Viricel, A., Gey, D., France, S.C., Boisselier, M.C., Samadi, S. (2015) Use of rad sequencing for delimiting species. *Heredity*, 114, 450–459. https://doi.org/10.1038/hdy.2014.105

Pante, E., Watling, L. (2012) *Chrysogorgia* from the New England and Corner Seamounts: Atlantic–Pacific connections. *Journal of the Marine Biological Association of the United Kingdom*, 92 (5), 911–927. https://doi.org/10.1017/S0025315411001354

Parimbelli, A. (2020) Invertebrate associations with deep-sea corals and sponges on the Irish Continental Margin. University of Padova. https://doi:10.13140/RG.2.2.19977.26726

Quattrini, A.M., Faircloth, B.C., Dueñas, L.F., Bridge, T.C.L., Brugler, M.R., Calixto-Botía, I.F., DeLeo, D.M., Forêt, S., Herrera, S., Lee, S.M.Y., Miller, D.J., Prada, C., Rádis-Baptista, G., Ramírez-Portilla, C., Sánchez, J.A., Rodríguez, E., McFadden, C.S. (2017) Universal target-enrichment baits for anthozoan (Cnidaria) phylogenomics: new approaches to longstanding problems. *Molecular Ecology Resources*, 18, 281–295. https://doi:10.1111/1755-0998.12736

Ronquist, F., Teslenko, M., Van Der Mark, P., Ayres, D.L., Darling, A., Höhna, S., Huelsenbeck, J.P. (2012) MrBayes 3.2: efficient Bayesian phylogenetic inference and model choice across a large model space. *Systematic Biology*, 61 (3), 539–542.

Rossi, S., Bramanti, L., Horta, P., Allcock, L., Carreiro-Silva, M., Coppari, M., Denis, V., Hadjioannou, L., Isla, E., Jimenez, C., Johnson, M., Mohn, C., Orejas, C., Ramšak, A., Reimer, J., Rinkevich, B., Rizzo, L., Salomidi, M., Samaai, T., Schubert, N., Soares, M., Thurstan, R.H., Vassallo, P., Ziveri, P., Zorrilla-Pujana, J. (2022) Protecting global marine animal forests. *Science*, 376, 929.

https://doi:10.1126/science.abq7583
Sánchez, J.A., Lasker, H.R., Taylor, D.J. (2003) Phylogenetic analyses among octocorals (Cnidaria): Mitochondrial and nuclear DNA sequences (lsu-rRNA, 16S and ssu-rRNA, 18S) support two convergent clades of branching gorgonians. *Molecular Phylogenetics and Evolution*, 29, 31–42. https://doi.org/10.1016/S1055-7903(03)00090-3
Tamura, K., Stecher, G., Kumar, S. (2021) MEGA11: molecular evolutionary genetics analysis version 11. *Molecular Biology and Evolution*, 38 (7), 3022–3027.
Untiedt, C.B., Quattrini, A.M., McFadden, C.S., Alderslade, P.A., Pante, E., Burridge, C.P. (2021) Phylogenetic relationships within *Chrysogorgia* (Alcyonacea: Octocorallia), a morphologically diverse genus of octocoral, revealed using a target enrichment approach. *Frontiers in Marine Science*, 7: 599984. doi: 10.3389/fmars.2020.599984
Versluys, J. (1902) Die Gorgoniden der Siboga-Expedition. 1. Die Chrysogorgiiden. *Siboga-Expeditie*, 13, 1–120.
Watling, L., Auster, P.J. (2021) Vulnerable marine ecosystems, communities, and indicator species: confusing concepts for conservation of seamounts. *Frontiers in Marine Science*, 8, 622586. https://doi: 10.3389/fmars.2021.622586
Xiang C., Gao F., Jakovlic, I., Lei, H. Hu, Y., Zhang, H., Zou, H., Wang, G., Zhang, D. (2023) Using PhyloSuite for molecular phylogeny and tree-based analyses. *iMeta,* e87. https://doi.org/10.1002/imt2.87.
Xu, Y., Zhan, Z., Li, Y., Xu, K. (2020) Morphology and phylogenetic analysis of two new species of deep-sea golden gorgonians (Cnidaria: Octocorallia: Chrysogorgiidae) from seamounts in the Western Pacific Ocean. *Zootaxa*, 4731 (2), 249–262. https://doi.org/10.11646/zootaxa.4731.2.4
Xu, Y., Zhan, Z., Xu, K. (2021a) Morphology and phylogeny of *Chrysogorgia pinniformis* sp. nov. and *C. varians* sp. nov., two golden corals from the Caroline seamounts in the tropical Western Pacific Ocean. *Journal of Oceanology and Limnology*, 39, 1767–1789. https://doi.org/10.1007/s00343-021-0386-5
Xu, Y., Zhan, Z., Xu, K. (2021b) Morphological and molecular characterization of five species including three new species of golden gorgonians (Cnidaria: Octocorallia) from seamounts in the Western Pacific. *Biology*, 10, 588. https://doi.org/10.3390/biology10070588
Xu, Y., Zhan, Z., Xu, K. (2023) Studies on western Pacific gorgonians (Anthozoa: Octocorallia, Chrysogorgiidae). Part 1: a review of the genus *Chrysogorgia*, with description of a new genus and three new species. *Zootaxa*, 5321 (1), 1–107. https://doi.org/10.11646/zootaxa.5321.1.1
Zhang, D., Gao, F., Jakovlić, I., Zou, H., Zhang, J., Li, W.X., Wang, G.T. (2020) PhyloSuite: An integrated and scalable desktop platform for streamlined molecular sequence data management and evolutionary phylogenetics studies. *Molecular Ecology Resources*, 20 (1), 348–355. https://doi: 10.1111/1755-0998.13096.

Supplementary

Table S1. Table of detailed statistics for the UCEs pipeline.
Figure S1. 90% tree of UCEs.